



Open Sea Operating Experience to Reduce Wave Energy Costs

Deliverable D3.2

Turbine-generator set laboratory tests in variable
unidirectional flow

Lead Beneficiary	Instituto Superior Técnico
Delivery date	2017-06-06
Dissemination level	Public
Status	Approved
Version	1.0
Keywords	Biradial turbine; Dry testing



This project has received funding from the European Union's Horizon 2020 research and innovation programme under grant agreement No 654444

Disclaimer

This Deliverable reflects only the author's views and the Agency is not responsible for any use that may be made of the information contained therein

Document Information

Grant Agreement Number	654444
Project Acronym	OPERA
Work Package	WP3
Task(s)	T3.2
Deliverable	D3.2
Title	Turbine-generator set laboratory tests in variable unidirectional flow
Author(s)	L.M.C. Gato; A.A.D. Carrelhas; F.X Correia da Fonseca; J.C.C. Henriques (IST)
File Name	OPERA_D3.2_Dry Testing_IST_2017-06-06_v1.0.docx

Change Record

Revision	Date	Description	Reviewer
0.1	05/01/2017	Initial outline	Authors
0.5	24/04/2017	Working draft	WP3 partners
0.9	05/06/2017	Reviewer comments updated	Coordinator
1.0	06/06/2017	Final version of deliverable for EC	EC



EXECUTIVE SUMMARY

This document represents Deliverable 3.2 (D3.2) of OPERA Work Package 3 (WP3): Power take-off reliability and performance, validation of new turbine.

This deliverable describes the laboratory tests performed at Instituto Superior Técnico (IST) in variable unidirectional flow of the novel biradial turbine which is a key innovation of the OPERA project. Laboratory test results cover a range of flow characteristics expected in open-sea operation.

This report addresses the following topics to document the performance characteristics, operating range specifications and assessment of CFD Model:

- ▶ **Efficiency tests results of the electrical generator** providing essential information to assess the turbine performance at the several testing stages: dry lab testing at IST, turbine testing in the Mutriku plant and turbine testing in the OCEANTEC offshore buoy.
- ▶ **Dry laboratory testing of the novel biradial turbine at IST** under constant and variable flow and constant and variable rotation speed.
- ▶ **Mechanical acceptance tests of the turbine-generator set and its high-speed safety valve** before shipping to the Mutriku plant.

Results from the biradial turbine dry tests showed that the experimental values for the efficiency are fairly close to those predicted by the CFD calculations, thus validating the turbine design method.



TABLE OF CONTENTS

EXECUTIVE SUMMARY	3
TABLE OF CONTENTS.....	4
LIST OF FIGURES.....	6
LIST OF TABLES.....	7
ABBREVIATIONS AND ACRONYMS.....	8
1. INTRODUCTION.....	9
2. BIRADIAL TURBINE MODEL TESTING	11
2.1 Experimental set-up.....	11
2.2 Results.....	13
2.2.1 Original design	13
2.2.2 Reinforced nozzle/difuser design	15
3. ELECTRICAL GENERATOR EFFICIENCY TESTS.....	17
3.1 Test rig and instrumentation	17
3.2 Experimental procedure	19
3.3 Data acquisition	20
3.4 Methodology.....	21
3.5 Results.....	22
4. OPERA TURBINE DRY TESTING	24
4.1 Test rig description	24
4.2 Signal acquisition	25
4.3 Air-flow valve	26
4.4 Steady-flow performance tests.....	28
4.4.1 Turbine flow-rate calibration.....	29
4.4.2 Performance curves	29
4.5 Random wave testing – Average efficiencies	31
4.5.1 Average efficiency in random waves: turbine rotation speed control.....	32
4.5.2 high speed safety Valve control algorithms	34
4.6 Mechanical integrity tests.....	35
4.6.1 Turbine vibration level.....	35
4.6.2 High-speed safety-valve.....	37





5. CONCLUSIONS 39

6. REFERENCES 40

APPENDIX A1: TURBINE VIBRATION TESTS 41

APPENDIX A2: HSSV PRELIMINARY TESTS 72

APPENDIX A3: MECHANICAL INTEGRITY TESTS 87



LIST OF FIGURES

Figure 1: 2.5 kW blow-down turbine test-rig of IST.	11
Figure 2: Experimental setup, showing the electrical generator, the horizontal-axis turbine and the plenum chamber. The diffuser is located inside the plenum chamber.	12
Figure 3: Efficiency of the biradial turbine model versus flow rate coefficient	14
Figure 4: Dimensionless plot of biradial turbine model pressure head versus flow rate (Original design).	14
Figure 5: Efficiency of the biradial turbine model versus flow rate coefficient	15
Figure 6: Test-rig for electrical generator efficiency measurements.	17
Figure 7: Electrical generator test rig and power electronics.	18
Figure 8: Current sensors calibration.....	19
Figure 9: Torque-meter calibration sensors.	19
Figure 10: Data acquisition system.....	20
Figure 11: Intrumentation board.....	21
Figure 12: Aron’s method for electrical power measurement.....	22
Figure 13: Current and voltage signals at the generator side (IBGRID).....	22
Figure 14: Current and voltage signals at the generator side (IBGen).	22
Figure 15: Electrical generator efficiency as a function of the rotation speed and power.	23
Figure 16: IST 55 kW V-FLOW turbine test rig representation.	25
Figure 17: Schematic representation of the IST 55 kW V-FLOW turbine test-rig.....	26
Figure 18: Schematic representation of the variable air-flow valve.	27
Figure 19: Variable air-flow valve.	27
Figure 20: IST V-FLOW turbine test-rig before turbine installation.....	28
Figure 21: OPERA biradial turbine being tested at IST.	28
Figure 22: Inlet turbine nozzle pressure drop versus flow rate.....	29
Figure 23: Dimensionless plot of biradial turbine efficiency versus flow rate.	30
Figure 24: Dimensionless plot of biradial turbine flow rate versus pressure head.....	30
Figure 25: Dimensionless plot of power output versus pressure head.....	31
Figure 26: unitary gaussian pressure spectrum.....	32
Figure 27: Imposed torque laws.	33
Figure 28: Turbine rotation speed for different torque laws.	33
Figure 29: Generator power for different torque laws.	34
Figure 30: Generator power for different HSSV control laws.	35
Figure 31: Vibration velocity (RMS) as a function of the turbine rotation speed without air flow.	36
Figure 32: Vibration velocity (RMS) for the turbine operating at 2500 rpm with air flow.....	36
Figure 33: High-speed stop-valve testing prior to turbine installation.	37



LIST OF TABLES

Table 1: Electrical generator and power electronics.	17
Table 2: Instrumentation for electrical generator efficiency tests.	18
Table 3: IST 55 kW V-Flow rig equipment.	25
Table 4: tested torque coefficients.	32
Table 5: Maximum RMS vibration velocity for constant as turbine rotation speed with variable air flow.	36



ABBREVIATIONS AND ACRONYMS

AMCA	Air Moving and Conditioning Association
CFD	Computational Fluid Dynamics
HSSV	High-Speed Safety Valve
OWC	Oscillating Water Column
PTO	Power Take Off System
WP	Work Package



1. INTRODUCTION

This document represents Deliverable 3.2 (D3.2) of OPERA Work Package 3 (WP3): Power take-off reliability and performance, validation of new turbine.

In this introduction some background information is provided setting the work of WP3 within the context of the OPERA project.

The air turbine driving an electrical generator is the essential component of the plant and where the wave-induced pneumatic energy is converted into useful electrical energy. The turbine is subject to much more demanding conditions than more conventional turbines (water, gas, steam, wind): the air flow rate is largely random, varies widely with sea state, and its direction is reversed twice in a wave cycle. Besides, the damping provided by the turbine should match what is required by the hydrodynamic process of wave energy absorption. Several types of self-rectifying air turbines have been proposed, and in some cases equipped OWC prototypes. The recently patented biradial air turbine has been found by numerical simulation and model testing to be the most efficient self-rectifying air turbine, apart from other advantages like its axial-compactness and capability to easily accommodate a fast acting air valve.

The overall aims of WP3 are to increase OWC turbine annual mean efficiency 50% and improve reliability of the PTO.

The turbine was designed to maximize the amount of energy absorbed from the waves, while taking into account its own rotation-speed-dependent aerodynamic efficiency and the efficiency of the electrical equipment under the widely varying sea states that characterize the local wave climate. The turbine-generator set was designed and constructed to be tested under real sea conditions, firstly at the fixed-structure Mutriku plant (where monitoring and adjustments can be done more easily) and later, under more demanding sea conditions, at offshore OCEANTEC Buoy.

Before shipping the turbine to the Mutriku plant the novel biradial turbine undergone a testing programme at Instituto Superior Técnico (IST) Turbomachinery Laboratory under constant and varying unidirectional flow to assess performance of the turbine and the electrical generator.

This deliverable addresses the following topics to document the performance characteristics, operating range specifications and assessment of CFD Model.

- ▶ **Efficiency tests results of the electrical generator** providing essential information to assess the turbine performance at the several testing stages: dry lab testing at IST, turbine testing in the Mutriku plant and turbine testing in the OCEANTEC offshore buoy.
- ▶ **Dry lab testing of the novel biradial turbine at IST** under constant and variable flow and at constant and variable speed.



- ▶ **Mechanical acceptance tests of the turbine-generator set and its high-speed safety valve (HSSV)** before shipping to the Mutriku plant.

This document outlines the tests performed at IST with the biradial turbine-generator set and its built-in high-speed safety valve, before its installation and testing in the Mutriku plant and in the offshore OCEANTEC floating device. The key sections of this deliverable are outlined below:

Section 2 presents the results of the turbine model testing at the 2.5 kW variable flow turbine test-rig for the original turbine design and the modified version with the large size struts located near the rotor inlet and exit that were needed as a consequence of the present OCEANTEC Buoy design that does not provide the most effective support for the biradial turbine.

Section 3 describes the tests performed with the 30 kW OPERA turbine electrical generator and its power electronics before the turbine integration to characterise the efficiency of the electrical generator and the power electronics when subjected to different values of rotation speed and torque.

Section 4 provides an overview of OPERA turbine dry testing performed at the IST 55 kW variable flow test rig, including the performance results obtained under steady-flow and for random flow with torque control, as well as the results of the mechanical integrity tests.

In **Section 5** conclusions are drawn based on the test results reported in this deliverable report and supporting analyses carried out within WP3.

2. BIRADIAL TURBINE MODEL TESTING

2.1 EXPERIMENTAL SET-UP

The aerodynamic design of the OPERA turbine was experimentally validated using a 0.488 m rotor diameter model of the OPERA turbine which was tested in unidirectional flow at the 2.5 kW blow-down turbine test-rig of IST that had been used before to model-test a variety of Wells turbines and axial-flow self-rectifying impulse turbines. The test rig is represented in Figure 1.

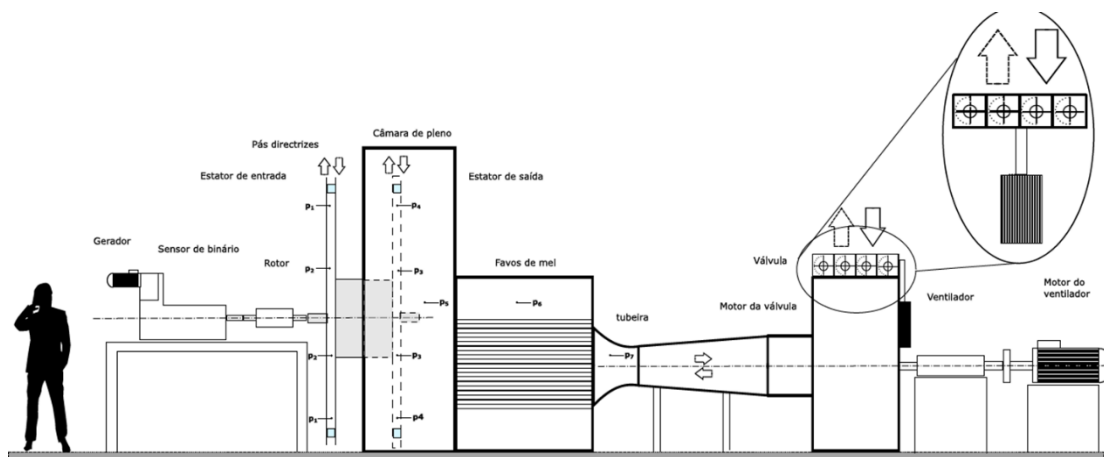


FIGURE 1: 2.5 KW BLOW-DOWN TURBINE TEST-RIG OF IST.

The pressure drop across the turbine was provided by a centrifugal fan and was operated by a variable speed controller which was connected to the fan motor. The induced air flow was directed through the turbine and then into a plenum chamber. The chamber contains a honeycomb lattice, which facilitates flow straightening prior to air entering a calibrated converging nozzle situated between the plenum chamber and the exhaust outlet. The plenum chamber and the nozzle were designed according to the Air Moving and Conditioning Association (AMCA) 210/67 standard. The 0.67 m-long nozzle contracts from 0.8 m to 0.4 m diameter, and the plenum chamber measured 2.00 m in length, 2.95 m in height and 2.95 m in width, see below. The turbine was connected, via a Datum Electronics torque-meter, to a motor-generator, which controlled the speed using a step-less variable speed controller. During operation, the motor-generator switched to either mode in order to maintain the chosen test speed.

The air valve attached to the radial fan consists of a set of rotating blades, which, depending of their position, regulate the air flow through the whole test-rig. All blades are attached to pivot handles which are interlinked by a rigid bar. The air valve is actuated by a linear motor which is coupled by a connecting rod to the pivot handles. The vertical translation of the linear motor imposes the rotation of the valve blades and consequently, depending on the direction of movement, the opening or closure of the air valve.

For each fan rotation speed, the air valve is calibrated in order to accurately reproduce the desired pressure inside the air chamber. By controlling the position of the linear motor, the developed algorithm is capable of reproducing irregular pressure spectra introduced by the user. Most importantly, taking into consideration the hydrodynamic coefficients of the Buoy/OWC chamber coupling, the devised algorithm is able to convert real sea wave climates, defined by wave energy spectra typical from the deployment location, into a pressure signal which is in turn accurately reproduced by the air-flow valve system.

The volume flow rate was determined by measuring the pressure drop in the pre-calibrated nozzle section, which was situated after the chamber. The turbine rotation speed was measured by a photo-electric speed pick-up. The recorded data included rotation speed, torque and pressure. The uncertainties in the measurements were estimated to be 0.1% of measured value for torque and rotation speed and 1% for air pressure relative to atmospheric pressure. The flow was assumed incompressible (constant density).

The rotor was fabricated of sintered nylon. Its diameter was 488 mm and the entrance/exit width was 53.7 mm. The 7 rotor blades were of constant thickness (equal to 3.7 mm), rounded at their inlet/ outlet edges. The radial gap between the rotor and the casing was about 1 mm. Two ball bearings on each side of the rotor supported the turbine shaft.

The inlet duct and the outlet duct (diffuser) of the turbine were formed by two pairs of flat steel discs, whose outer edges were rounded. Each pair of discs holds the guide vanes. The guide vanes were made of polyurethane with the use of silicone moulds.



FIGURE 2: EXPERIMENTAL SETUP, SHOWING THE ELECTRICAL GENERATOR, THE HORIZONTAL-AXIS TURBINE AND THE PLENUM CHAMBER. THE DIFFUSER IS LOCATED INSIDE THE PLENUM CHAMBER.

2.2 RESULTS

2.2.1 ORIGINAL DESIGN

Experimental results are plotted, in dimensionless form, in Figure 3 to Figure 5 together with results from the computational fluid dynamics (CFD) code FLUENT that solves the three-dimensional Reynolds-averaged Navier-Stokes equations with a $k-\omega$ SST turbulence model. Details of the computations can be found in (Carrelhas, 2017). The plotted experimental results concern a range of rotation speeds between 150 and 1,000 rpm ($6 \times 10^4 \leq \text{Re} \leq 4 \times 10^5$). The mechanical losses (due to bearing friction and aerodynamic friction on the rotor outer walls) were measured separately and the corresponding values were added to the torque T measured from the electrical power; this means that the efficiency computed from the experimental results is in fact an inner aerodynamic efficiency.

The dimensionless quantities plotted in in Figure 3 to Figure 5 are defined as follows:

$$\Phi = \frac{Q}{\omega D^3} \quad (\text{flow coefficient}), \quad (1)$$

$$\Psi = \frac{p}{\rho \omega^2 D^2} \quad (\text{pressure head coefficient}), \quad (2)$$

$$\Pi = \frac{T}{\rho \omega^2 D^5} = \frac{P}{\rho \omega^3 D^5} \quad (\text{power coefficient}), \quad (3)$$

$$\eta = \frac{P}{Q \Delta p} \quad (\text{efficiency}). \quad (4)$$

Here, Q is volume flow rate, p is pressure head (difference between atmospheric pressure and pressure in the plenum chamber at turbine exit), D is rotor diameter, ρ is air density, ω is rotation speed in radians per unit time, T is torque and $P = \omega T$ is power output. It should be noted that the efficiency is defined here as total-to-static efficiency.



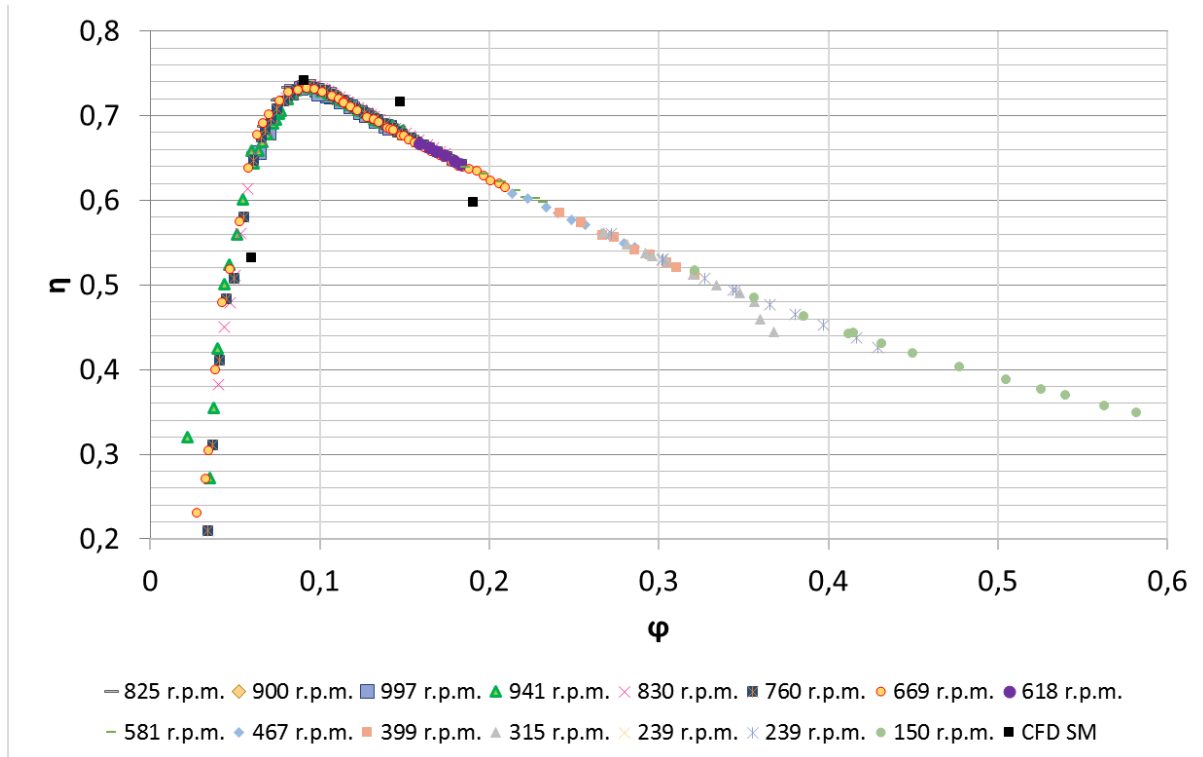


FIGURE 3: EFFICIENCY OF THE BIRADIAL TURBINE MODEL VERSUS FLOW RATE COEFFICIENT (ORIGINAL DESIGN).

In Figure 3, the CFD results show that the predicted efficiency of the turbine is fairly close to the experimental values, thus validating the turbine design method. The measured efficiencies reach a peak about 0.73 at $\Phi \cong 0.09$.

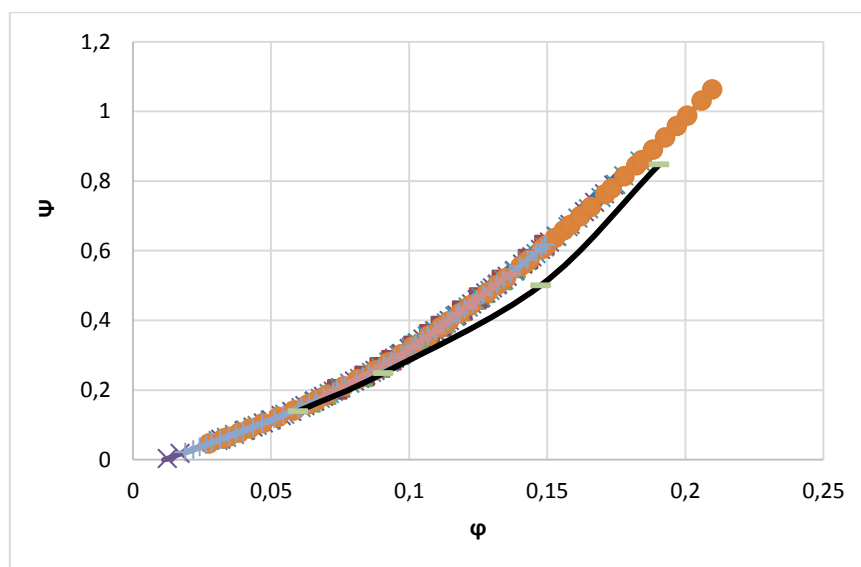


FIGURE 4: DIMENSIONLESS PLOT OF BIRADIAL TURBINE MODEL PRESSURE HEAD VERSUS FLOW RATE (ORIGINAL DESIGN).

Figure 4 shows that the pressure-versus-flow-rate relationship exhibited by the biradial turbine, unlike the Wells turbine, is far from linear (it is more nearly quadratic), a characteristic shared with self-rectifying axial-flow turbines of impulse type (see (Falcao & Gato, 2012)).

2.2.2 REINFORCED NOZZLE/DIFUSER DESIGN

The present design of OCEANTEC Buoy did not provide the most appropriate support for the installation of a biradial turbine. A much simpler and lighter biradial turbine could have been produced if the design of the wave energy converter had considered the integration of the turbine from the very beginning. As a consequence of the high values of pressure differences specified in the design requirements provided by OCEANTEC, the original design was modified to incorporate a number of very large size struts located near the rotor inlet and exit. The detrimental effect of these large struts was assessed by testing the modified version of the biradial turbine model.

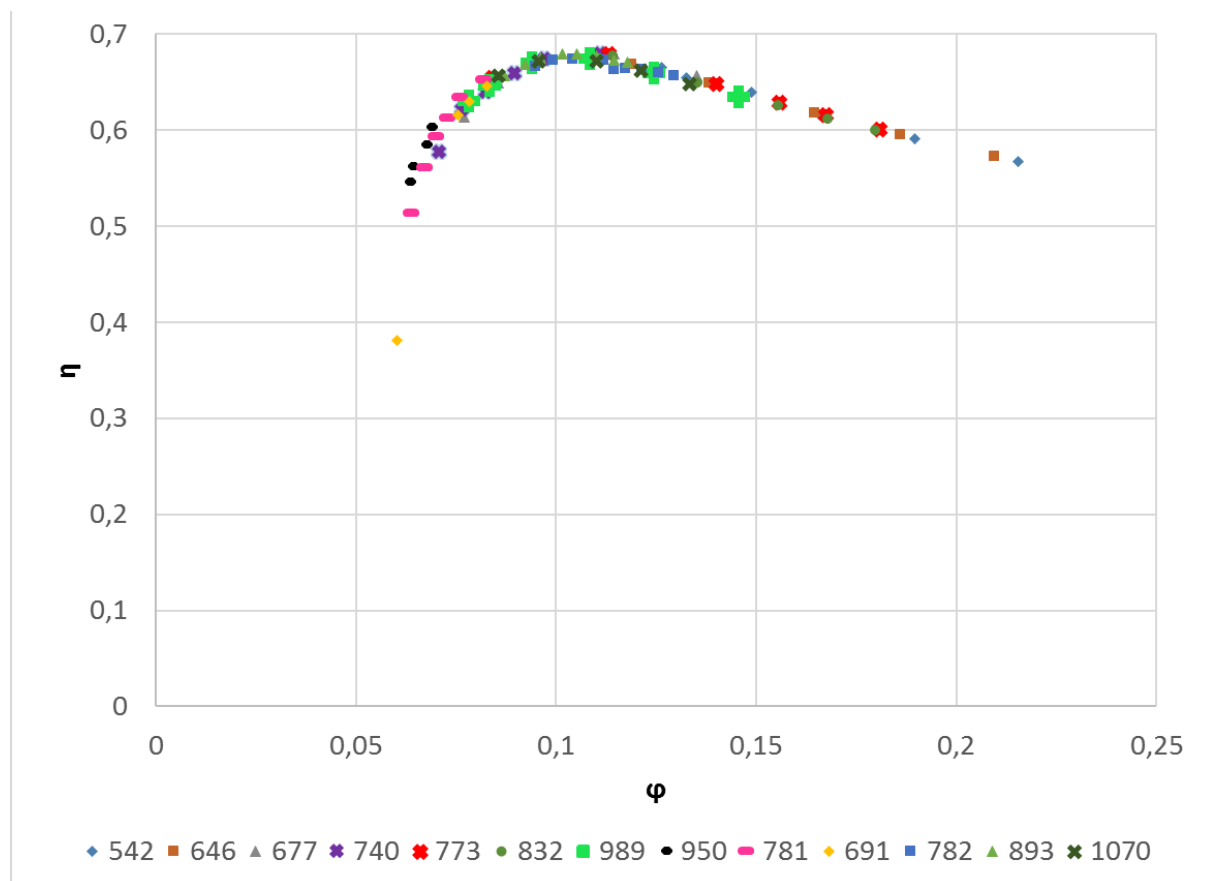


FIGURE 5: EFFICIENCY OF THE BIRADIAL TURBINE MODEL VERSUS FLOW RATE COEFFICIENT (REINFORCED NOZZLE/DIFUSER DESIGN).

Figure 5 shows the detrimental effect of the large size of the nozzle/diffuser struts required for the present design of the OPERA turbine. The measured efficiencies reach a peak about

0.67 at $\Phi \cong 0.11$ whereas in the original design the peak efficiency is about 0.73 at $\Phi \cong 0.09$.

This detrimental effect can be easily avoided in future designs if the floating wave energy converter design takes into account the integration of the biradial turbine large nozzle/diffuser from the very beginning.



3. ELECTRICAL GENERATOR EFFICIENCY TESTS

The current investigation involved the measurement of the electrical power produced by the 30 kW OPERA turbine-electrical-generator set both at the exit of the electrical generator and at the exit of its power electronics, to characterise the efficiency of the electrical generator and of the power electronics when subjected to different values of rotation speed and torque.

The OPERA turbine electrical generator and the power electronics are listed in Table 1.

TABLE 1: ELECTRICAL GENERATOR AND POWER ELECTRONICS.

Description	Reference	Power (kW)
SIEMENS IEC Squirrel-Cage Low-Voltage Electrical Machine	1LE1603-2AB53-4GB4-Z, Options: G01+H07+H20+L06+N10+N31 +Q02+Q63+Q78+S04	30
SINAMICS G120 Regenerative Power Module PM250	6SL3225-0BE33-0AA0	30
SINAMICS G120 Control Unit CU250S-2	6SL3255-0AA00-4CA1	-

3.1 TEST RIG AND INSTRUMENTATION

The test rig is represented in Figure 6 and Figure 7.

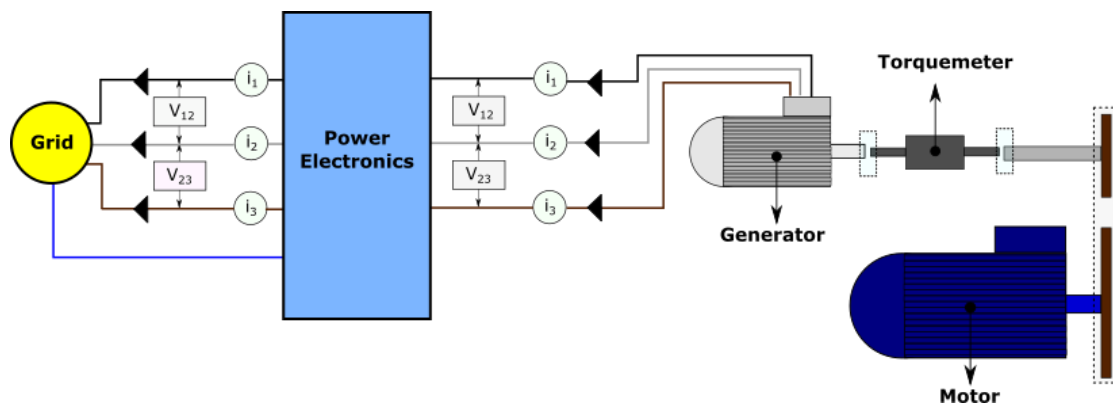


FIGURE 6: TEST-RIG FOR ELECTRICAL GENERATOR EFFICIENCY MEASUREMENTS.



FIGURE 7: ELECTRICAL GENERATOR TEST RIG AND POWER ELECTRONICS.

The OPERA turbine electrical generator was driven by a three phase 160 kW variable speed induction motor via a transmission system incorporating a torque-meter through semi-rigid couplings. The generator was connected to the power electronics through a power cable (PCG) with four conductors: three phases and one ground. The power electronics was connected to the electrical grid through a similar power cable (PCPW). Both PCG and PCPW cables have incorporated Hall-effect current transducers at each phase and two voltage transducers connected in parallel between two phases. The electrical generator power electronics could be parametrized either in speed control or in torque control.

The maximum rotation speed and turbine shaft torque were set to 3000 rpm and 120Nm, respectively. The nominal current and voltage of the electrical generator are 55 A and 480 V, respectively. The instrumentation was selected to meet the required ranges, as shown in Table 2.

TABLE 2: INSTRUMENTATION FOR ELECTRICAL GENERATOR EFFICIENCY TESTS.

Instrument	Variable to measure	Range
Vibrometer torquemeter	torque	0-200 Nm
Current transducer HAS 200-S	current	0-200 A
Voltage transducer LV25-P	voltage	0-500 V

All the instrumentation was calibrated at IST. The calibration of torque transducer was performed on a calibrated lever arm using a set of calibrated masses. The current and voltage transducers were calibrated using high accuracy ammeters and voltmeters. Figure 8 and Figure 9 show the calibration of current and torque transducer.



FIGURE 8: CURRENT SENSORS CALIBRATION.



FIGURE 9: TORQUE-METER CALIBRATION SENSORS.

3.2 EXPERIMENTAL PROCEDURE

A predetermined rotation speed and torque were set, respectively, to the electrical motor and to the electrical generator. For each pair of values, measurements of torque, rotation speed, current and voltage were made. The rotation speed was set directly to the frequency converter of the electrical motor by a potentiometer and the torque was set in the control

unit of the electrical generator power electronics as an analogue input with a range of 0-10 V, which corresponds to 0-120 Nm. The direction of the rotation was set to be opposite to the direction of the imposed torque.

3.3 DATA ACQUISITION

Figure 10 presents an overview of the data acquisition system. The data acquisition system is composed by two National instruments PCI-6221 boards, two instrumentation boards (see Figure 11) and the torque transducer interface.

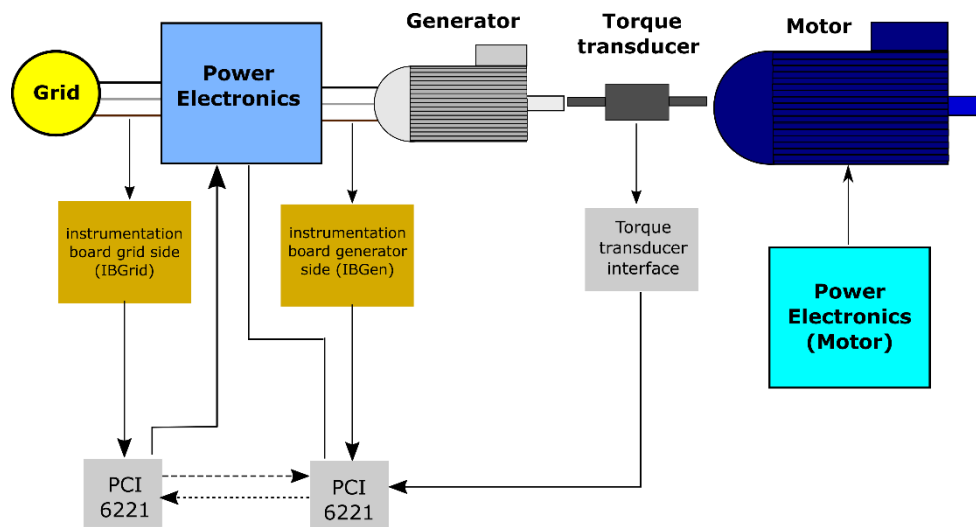


FIGURE 10: DATA ACQUISITION SYSTEM.

The instrumentation boards consist of the power supply to the current and voltage transducers, the reading system of the voltage transducers and a RJ45 port. One of them is dedicated to the measurements of signals at the generator side (IBGen) and the other one for the grid side (IBGrid).

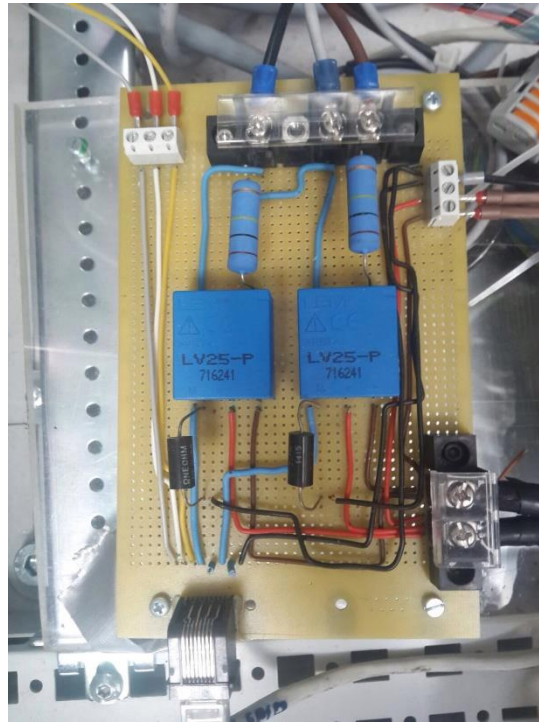


FIGURE 11: INSTRUMENTATION BOARD.

A torque transducer interface is used for the torque reading and its transmission to the DAQ system.

A routine with MATLAB communicates with the PCI-6221 boards to impose the required torque to the generator via one of analogue output ports and save the corresponding acquired torque-meter data. A digital trigger was set at the beginning of each test to synchronize the data acquisition of the two PCI-6221 boards.

The frequency rate was set to 62500 Hz, which is the maximum permitted by the DAQ system for analogue inputs. A lower frequency rate would lead to results with aliasing and wrong calculations.

All signals that enter and exit the DAQ system are transmitted through shield ethernet cable to ensure the minimum noise introduction in the signal.

3.4 METHODOLOGY

The electrical power from the generator, P_G , and power electronics, P_{pW} , are calculated with the Aron's Method. This method states that the active power absorbed by a three-wire AC system can be calculated by measuring the current in phase 1, i_1 , and 3, i_3 , and the voltage between phase 1 and 2, V_{12} , and 2 and 3, V_{23} , and is given by

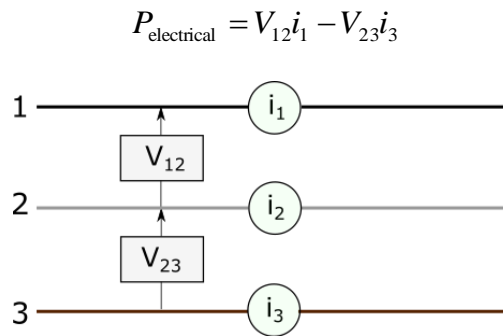


FIGURE 12: ARON'S METHOD FOR ELECTRICAL POWER MEASUREMENT.

The shaft power is $P_{\text{shaft}} = T\Omega$, where T is the measured torque and Ω is the measured rotation speed.

The efficiency of the electrical generator is then $\eta_G = P_G / P_{\text{shaft}}$ and efficiency of power electronics is $\eta_{\text{pW}} = P_{\text{pW}} / P_G$.

3.5 RESULTS

Signals from IBGrid and IBGen need special attention. Figure 13 and Figure 14 show in blue signals from current and voltage from IBGrid and IBGen.

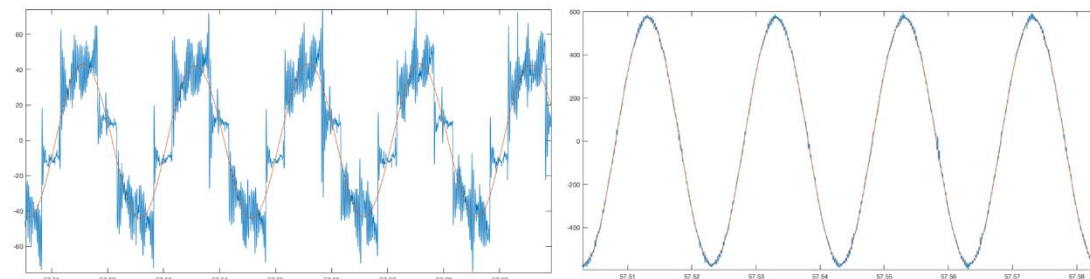


FIGURE 13: CURRENT AND VOLTAGE SIGNALS AT THE GENERATOR SIDE (IBGRID).

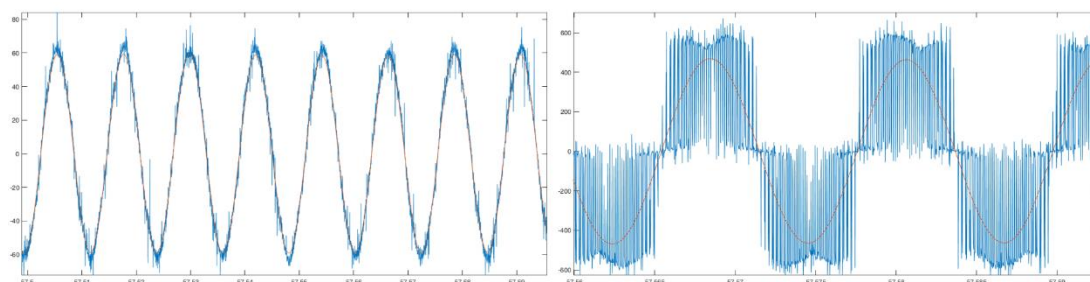


FIGURE 14: CURRENT AND VOLTAGE SIGNALS AT THE GENERATOR SIDE (IBGEN).



These signals need to be filtered so that the electrical power is calculated in a proper way. A variant of Savitzky-Golay filter was used and the results are shown in orange in Figure 13 and Figure 14. Results from calibration are represented in Figure 15.

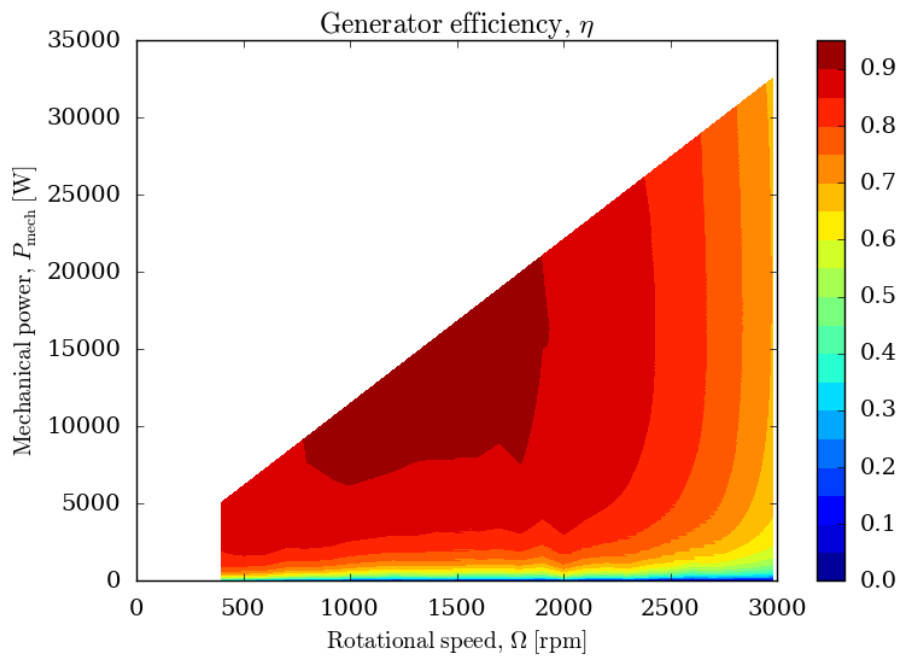


FIGURE 15: ELECTRICAL GENERATOR EFFICIENCY AS A FUNCTION OF THE ROTATION SPEED AND POWER.

Results in Figure 15 show that, although the electrical generator achieves very high efficiency in a wide range of rotation speeds and power, sharp drop of efficiency is observed for low power and low rotation speed. Furthermore, it is observed that the efficiency of the electrical generator decreases significantly for rotation speeds above 2,300 rpm.

4. OPERA TURBINE DRY TESTING

Experimental testing is a fundamental step in turbine development, despite the sharp increase in available computational power and improvements on CFD models over the last few years. In contrast to conventional turbines which are traditionally designed for steady-state operating conditions, self-rectifying air turbines devised for wave energy extraction are by definition exposed to oscillating air flows. The ability to experimentally test these turbines under irregular air flows and, most importantly, under real operating conditions is far-reaching.

4.1 TEST RIG DESCRIPTION

The IST V-Flow Turbine Lab is a test-rig designed to experimentally test air turbines under unidirectional variable flows. Given that the biradial turbine is symmetric, the turbine response is independent to the direction of the flow and therefore testing exclusively under unidirectional flows is sufficient. The variable flows are accurately reproduced with a calibrated air flow valve connected to the radial fan which is forcing the air through the turbine.

The test-rig is comprised by eight major components. Firstly, the OPERA biradial turbine was supplied with a horizontal adapting antechamber (1) whose purpose is to connect the turbine to the available vertical air duct in the Mutriku plant. This antechamber is also used in this test-rig to guide the air flow from the biradial turbine to the first plenum chamber at low speeds. The first plenum chamber (2) is designed to significantly reduce the air speed and swirl motions which impairs the correct pressure measurement. Connected to the first plenum, there is a honeycomb flow-straightener (3) required to further minimize the air swirl. Downstream, a calibrated flow nozzle (4) measures the air flow rate through the differential pressure principle. The air flows then into a diffuser (5) designed to recover kinetic energy. The diffuser is subsequently connected to a second plenum chamber (6). This second plenum chamber was devised not only to work as an elbow and connect to a duct at the ground level but also to smooth out any pressure wave that might be produced by the rapid closure of the high-speed valve. Lastly, the air flow rate and pressure gradient are imposed by a 55 kW radial fan (7) that is connected the plenum (2) and controlled by a frequency converter. Downstream of the radial fan, before being discharge onto the atmosphere, the air is driven through an automated air valve (8) which is able to accurately reproduce pressure signals imposed by a computer.

The designs of the plenum chambers, flow nozzle and diffuser were performed in accordance with the AMCA 210-99 Standards for experimental turbine testing.



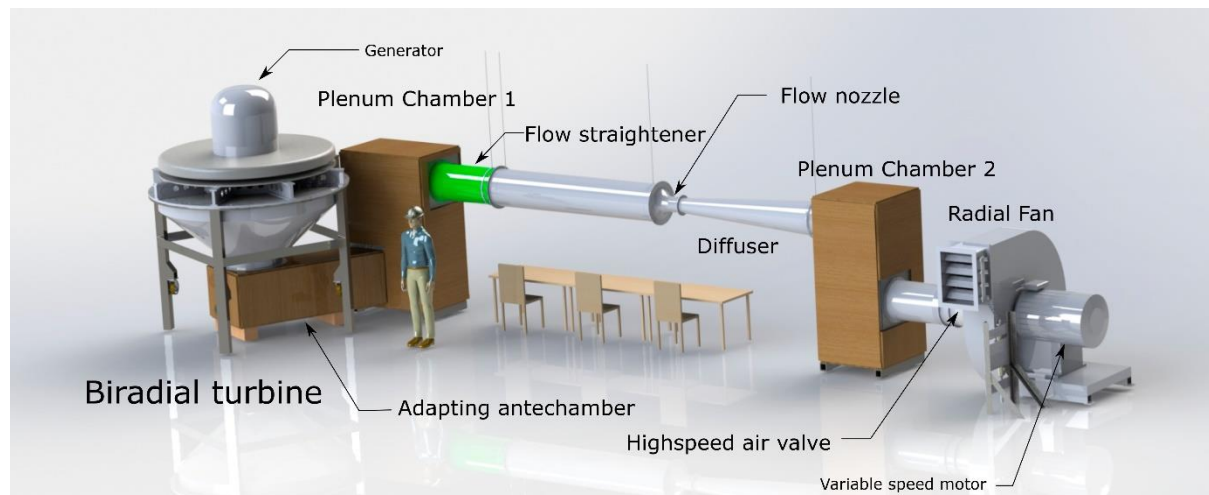


FIGURE 16: IST 55 KW V-FLOW TURBINE TEST RIG REPRESENTATION.

4.2 SIGNAL ACQUISITION

Throughout the experimental testing, several signals are being acquired. The differential pressure at the nozzle together with the air atmospheric pressure and temperature are being acquired in order to calculate the instantaneous air flow rate. The radial fan rotation speed is being controlled by a variable frequency drive. Together with the position control of the air valve attached to the discharge side of the radial fan, the fan's pressure head and air flow rate are imposed by a control algorithm.

In respect to the biradial turbine, the static pressure is measured on six different locations. On each stator (entry and exit), the pressure is measured firstly near to the stator external diameter and secondly close to the turbine rotor. At the conical adapter, two static pressure plugs measure the turbine pressure drop. The turbine-generator is then controlled either in rotation speed or torque through an analogic signal, which subsequently allows advanced control strategies for average power output maximization. For turbine vibration monitoring, two accelerometers are coupled to the turbine structure and the data signal is acquired.

The OPERA biradial turbine is equipped with a High-Speed Safety Valve (HSSV) for turbine protection and latching control purposes, which is actuated by four electric linear actuators. The control of the HSSV is accomplished by a developed control algorithm.

TABLE 3: IST 55 KW V-FLOW RIG EQUIPMENT.

Component	Power	Reference
Radial Fan	55 kW	METEC FI 801 N4 55 KW
Variable-frequency drive	55 kW	ABB ACS550-01-125A-4
Linear Motor	-	LINMOT P01-48x360F/480x630

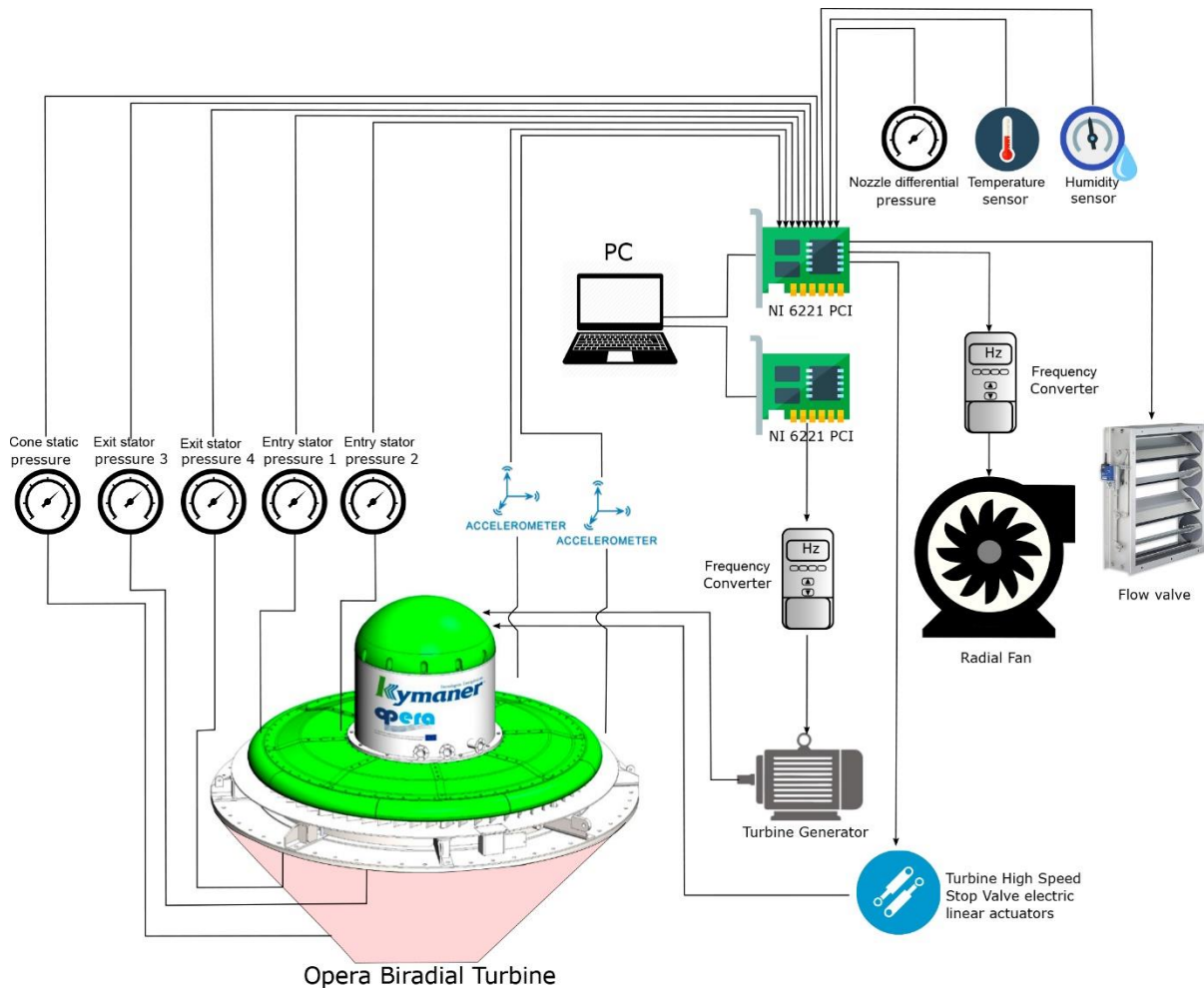


FIGURE 17: SCHEMATIC REPRESENTATION OF THE IST 55 KW V-FLOW TURBINE TEST-RIG.

4.3 AIR-FLOW VALVE

The air valve attached to the radial fan consists of a set of rotating blades, which, depending of their position, regulate the air flow through the whole test-rig. All four blades are attached to pivot handles which are interlinked by a rigid bar. The air valve is actuated by a linear motor which is coupled by a connecting rod to the pivot handles. The vertical translation of the linear motor imposes the rotation of the valve blades and consequently, depending on the direction of movement, the opening or closure of the air valve.

For each fan rotation speed, the air valve is calibrated in order to accurately reproduce the desired pressure inside the conical air chamber. By controlling the position of the linear motor, the developed algorithm is capable of reproducing irregular pressure spectra introduced by the user. Most importantly, taking into consideration the hydrodynamic coefficients of the Buoy/OWC chamber coupling, the devised algorithm is able to convert real sea wave climates, defined by wave energy spectra typical of the deployment location, into a pressure signal which is in turn accurately reproduced by the air-flow valve system.

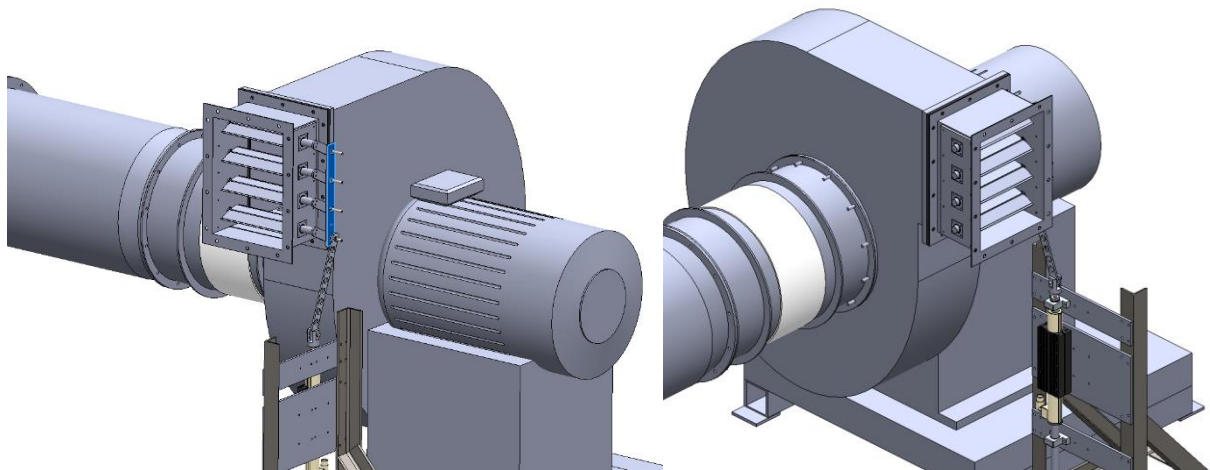


FIGURE 18: SCHEMATIC REPRESENTATION OF THE VARIABLE AIR-FLOW VALVE.



FIGURE 19: VARIABLE AIR-FLOW VALVE.



FIGURE 20: IST V-FLOW TURBINE TEST-RIG BEFORE TURBINE INSTALLATION.

4.4 STEADY-FLOW PERFORMANCE TESTS

The turbine arrived at IST on 7th April. The turbine was then installed in the dry test rig and all the sensors were connected. Data acquisition was ready on 12th April.



FIGURE 21: OPERA BIRADIAL TURBINE BEING TESTED AT IST.

4.4.1 TURBINE FLOW-RATE CALIBRATION

In real operational conditions, turbine flow rate can be calculated from the calibration of the inlet nozzle pressure drop. Calibration results are shown in Figure 22. As should be expected the inlet nozzle pressure drop is independent of the turbine rotation speed.

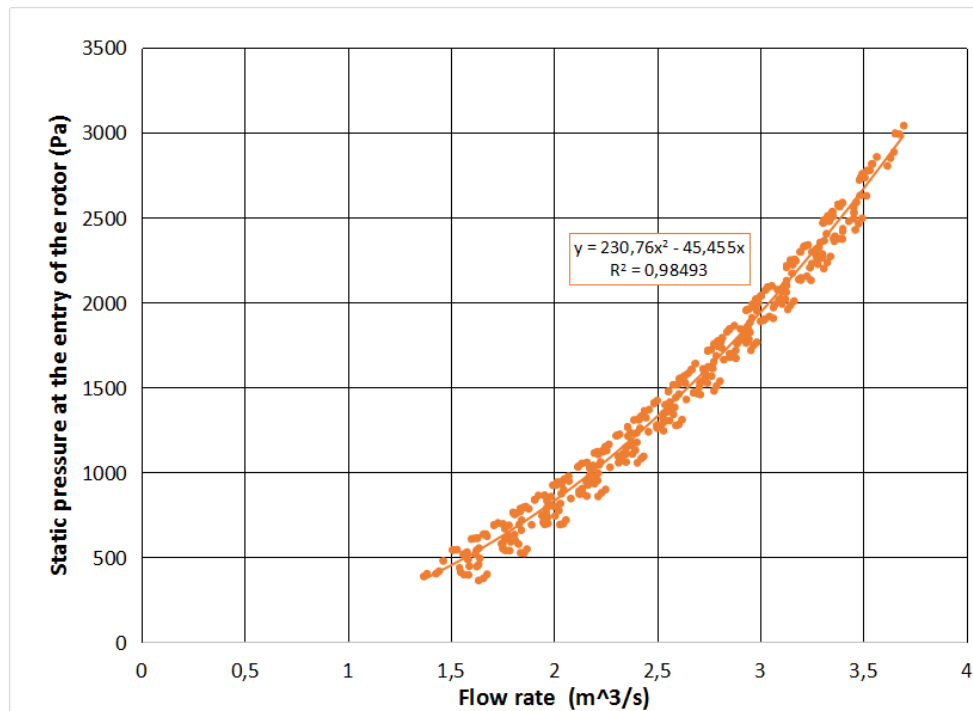


FIGURE 22: INLET TURBINE NOZZLE PRESSURE DROP VERSUS FLOW RATE.

4.4.2 PERFORMANCE CURVES

Experimental results are plotted, in dimensionless form, in Figure 23 to Figure 25. The plotted experimental results concern a range of rotation speeds between 598 and 2,218 rpm ($2.4 \times 10^5 \leq Re \leq 8.8 \times 10^5$). The mechanical losses (due to bearing friction and aerodynamic friction on the rotor outer walls) were measured separately at zero flow rate and the corresponding values were added to the torque T measured from the electrical power; this means that the efficiency computed from the experimental results is in fact an inner aerodynamic efficiency.

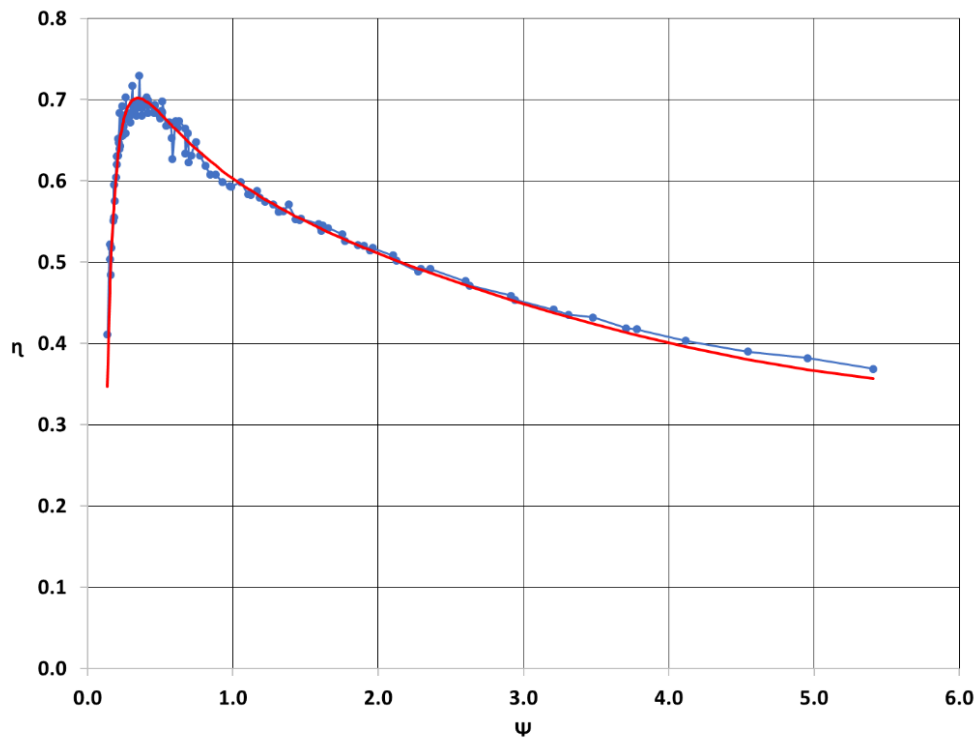


FIGURE 23: DIMENSIONLESS PLOT OF BIRADIAL TURBINE EFFICIENCY VERSUS FLOW RATE.

The scatter in experimental points in Figure 23 may be explained by the wide range of rotation speeds at which the tests were run. The measured efficiencies reach a peak about 0.68 at $\Phi \cong 0.11$.

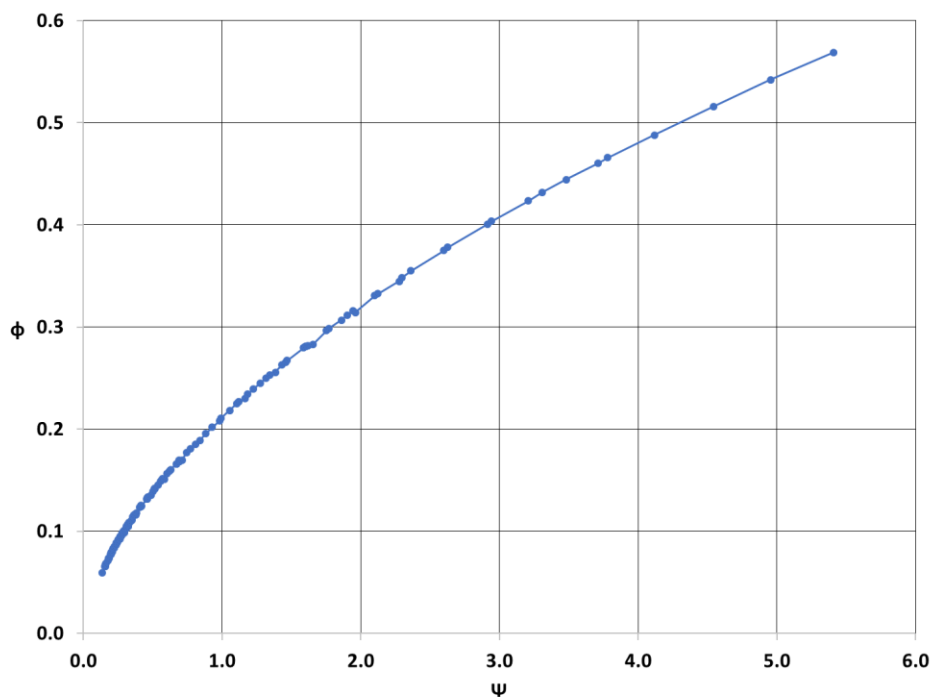


FIGURE 24: DIMENSIONLESS PLOT OF BIRADIAL TURBINE FLOW RATE VERSUS PRESSURE HEAD.

Figure 24 shows that the pressure-versus-flow-rate relationship exhibited by the biradial turbine, unlike the Wells turbine, is far from linear (it is more nearly quadratic), a characteristic shared with self-rectifying axial-flow turbines of impulse type (see (Falcao & Gato, 2012)).

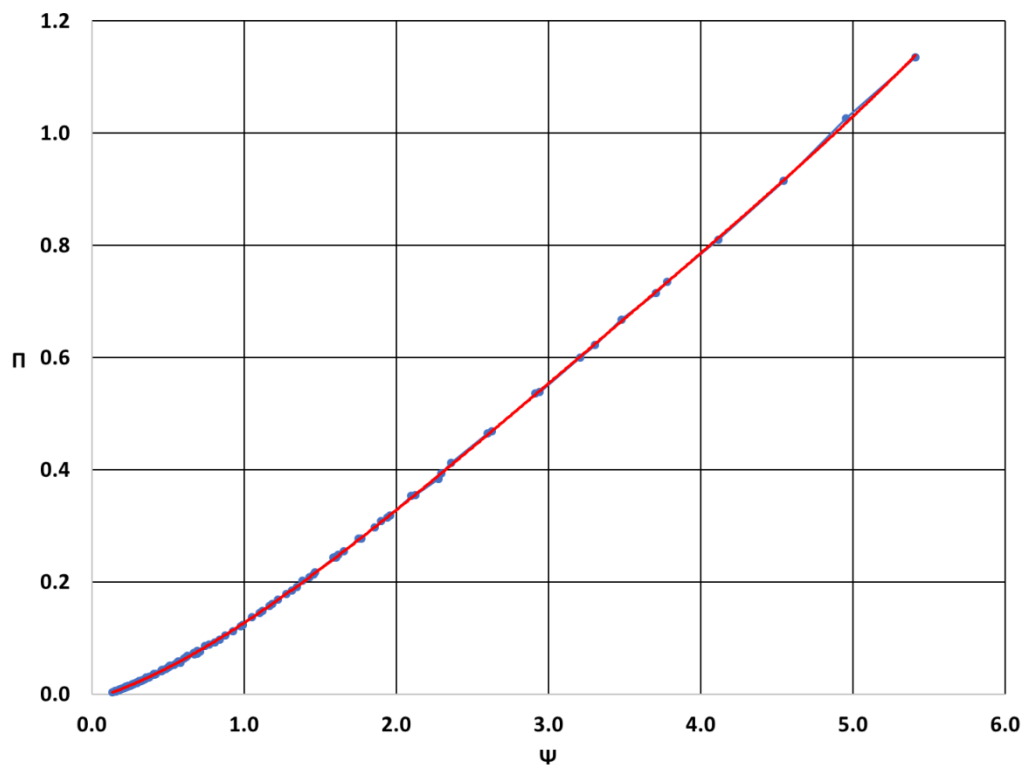


FIGURE 25: DIMENSIONLESS PLOT OF POWER OUTPUT VERSUS PRESSURE HEAD.

Figure 25 shows that the power output of the biradial turbine increases with flow rate, even for very large values of Ψ . This does not happen with the Wells turbine, where the power output and the efficiency drop sharply when the flow rate exceeds the limit of stall-free conditions at the rotor blades (see (Falcao & Gato, 2012)).

4.5 RANDOM WAVE TESTING – AVERAGE EFFICIENCIES

Given the random characteristics of the sea waves oscillations, self-rectifying air turbines devised for wave energy extraction are by definition exposed to randomly oscillating air flows. In order to characterize the turbine under randomly oscillating air flows, several pressure spectra were reproduced in the V-Flow Turbine Lab. Each pressure spectrum was defined with a generic Gaussian curve shape, with a spectrum peak for the period of 9 seconds and a frequency standard deviation of 0.02 Hz, for different pressure RMS values.

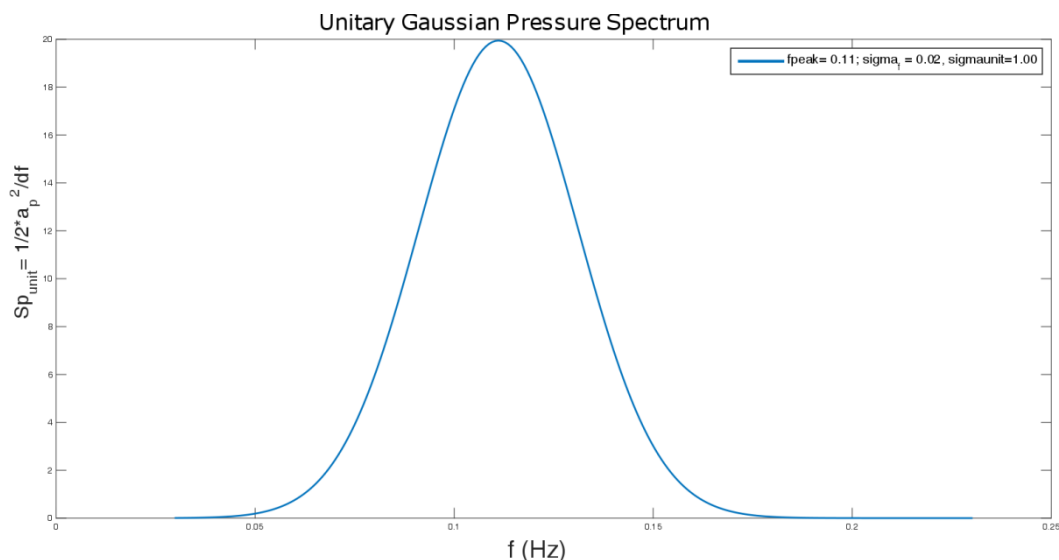


FIGURE 26: UNITARY GAUSSIAN PRESSURE SPECTRUM.

4.5.1 AVERAGE EFFICIENCY IN RANDOM WAVES: TURBINE ROTATION SPEED CONTROL

In normal operating conditions, the OPERA biradial turbine is controlled in torque mode. During the tests, three torque laws were tested and implemented for the same introduced pressure spectrum. In order not to exceed the generator rated power and maximum rotation speed, constraining control laws were also developed.

For steady flow conditions, the power coefficient $\Pi_{optimal}$ that maximizes the turbine efficiency was determined. For irregular flow conditions, a first assumption of the optimal torque law, that maximizes the power extraction of the turbine-generator coupling for each turbine speed, was defined as

$$T = \Pi_{optimal} \rho \Omega^2 D^5 = a \Omega^b,$$

Two other torque laws were tested for smaller and larger values of torque coefficient a , as presented below in Table 4: tested torque coefficients.

TABLE 4: TESTED TORQUE COEFFICIENTS.

Torque law	$a \times 10^3$ [kg m ²]	b [-]
1	1.11	2
2	0.557	2
3	2.23	2

The reproduced torques and turbine speeds points as well as the introduced control laws for the three tests are represented in Figure 27. The presented plots consist of unfiltered data. Major deviations from the introduced torque law lines can be explained by the statistical

uncertainty caused by unfiltered signal noise. Nonetheless, the impacts of changing the torque law coefficients are clear.

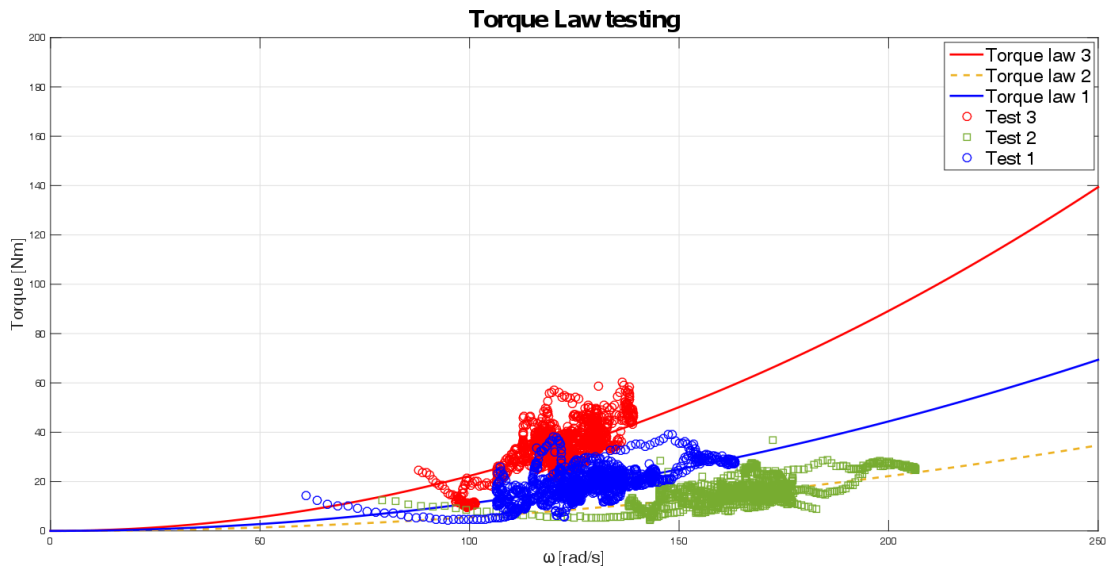


FIGURE 27: IMPOSED TORQUE LAWS.

As expected, in comparison to torque law 1, an increase in a (as defined by curve 3) produced larger torques for the same speed, which resulted in lower turbine rotation speeds on average (see Figure 28). On the other hand, smaller values of a allowed the turbine to rotate more freely, which lead to larger rotation speeds and lower power extraction efficiency.

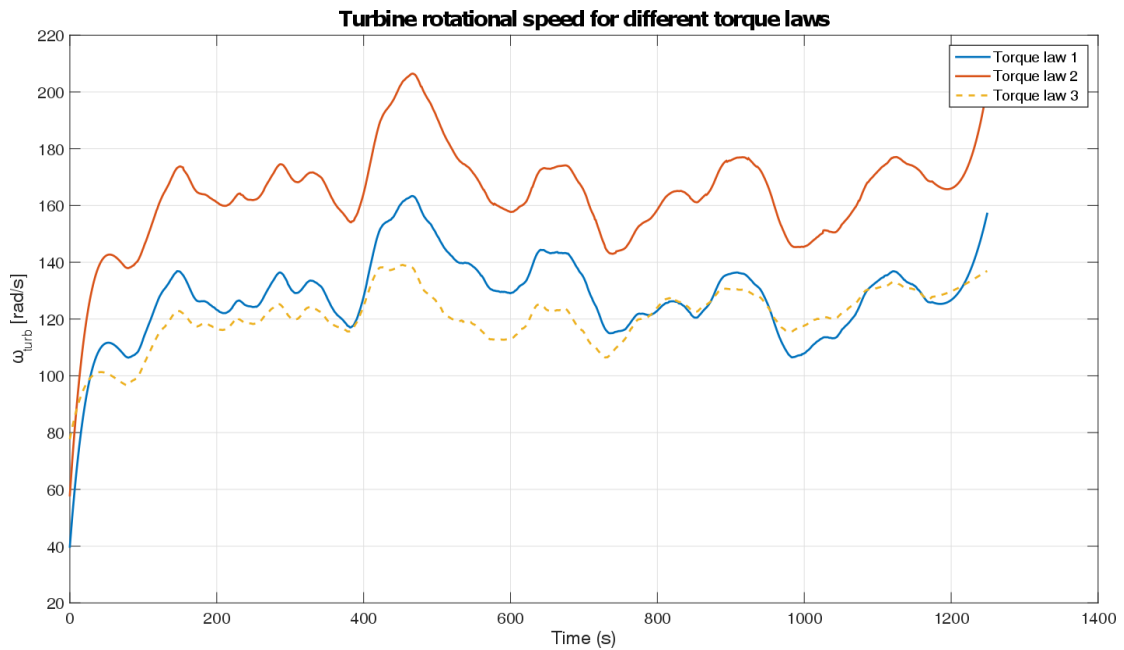


FIGURE 28: TURBINE ROTATION SPEED FOR DIFFERENT TORQUE LAWS.

While Torque law no.3 reduced the rotation speeds, Torque law no.2 reduced the extracted power, as a result of moving away from the optimal torque conditions. A combination of such strategies can be implemented for safety purposes in the event of extreme wave conditions in order to avoid excessive rotation speeds or powers respectively.

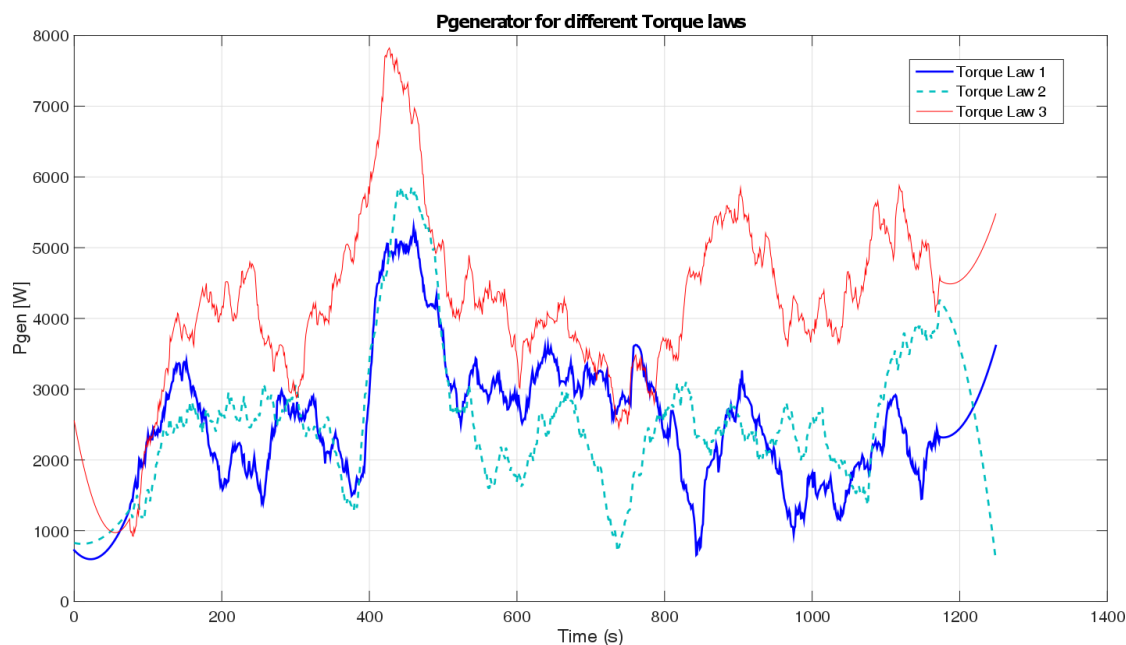


FIGURE 29: GENERATOR POWER FOR DIFFERENT TORQUE LAWS.

4.5.2 HIGH SPEED SAFETY VALVE CONTROL ALGORITHMS

High-Speed Safety Valve (HSSV) control algorithms were designed to actuate the valve whenever necessary to avoid excessively large rotation speeds. The control conditions were defined. The maximum rotation speed was set to 160 rad/s. In the event of speed limit being exceeded, the HSSV was programmed to close completely until the turbine decelerated to 100 rad/s.

Three HSSV control algorithms were tested. A linear control law, represented as a grey dashed line, and two quadratic laws represented in blue and red. The linear law, as the name suggests, considered a linear pressure response to the valve closure percentage. The two considered quadratic laws differed just in degree of response aggressiveness.

An optimal HSSV control algorithm (depicted as a red line) was obtained, which successfully avoided the excessive turbine speeds.

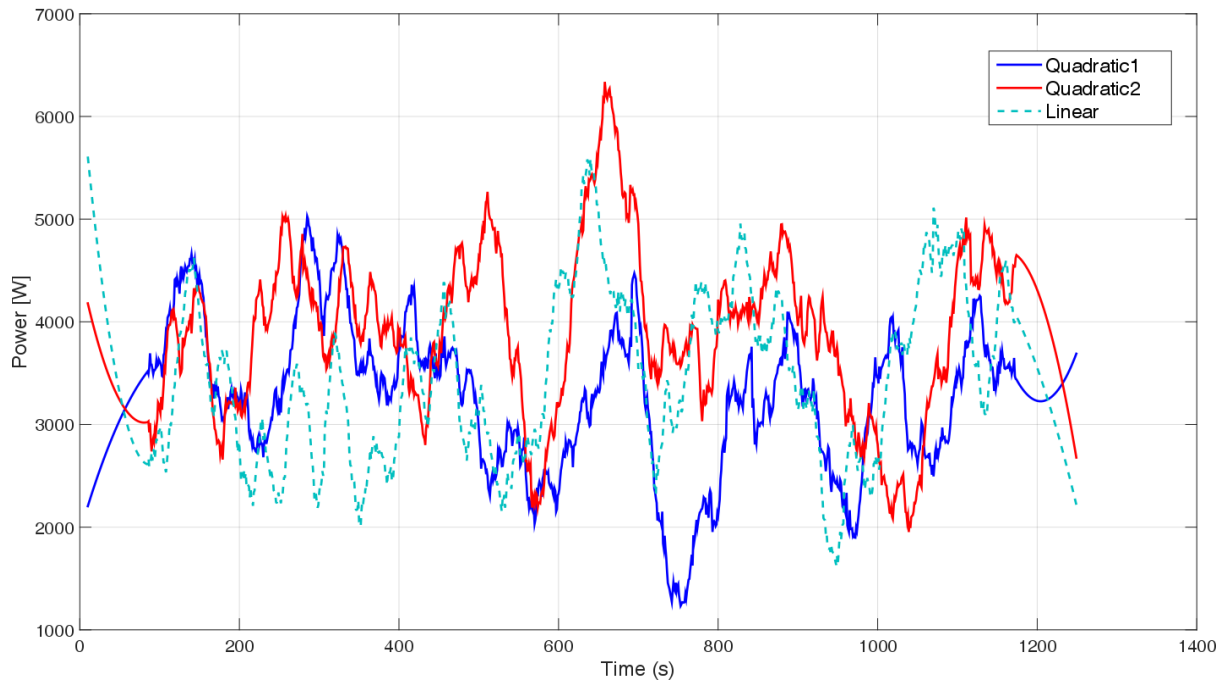


FIGURE 30: GENERATOR POWER FOR DIFFERENT HSSV CONTROL LAWS.

4.6 MECHANICAL INTEGRITY TESTS

4.6.1 TURBINE VIBRATION LEVEL

The objective of the mechanical integrity tests was to identify any vibration problems which may lead to an early turbine failure in different operating conditions.

The following tests were performed by a certified company when the turbine was installed at the IST test rig. Results of the above tests are fully reported in APPENDIX A1.

4.6.1.1 TEST 1A: VIBRATION CONTROL IN THE RANGE OF ROTATION SPEEDS WITHOUT AIRFLOW

The turbine is running using the generator as a motor. A slow 10 minutes ramp up from 0 to 2,500 rpm followed by a slow 10 minutes ramp down from 2,500 rpm to 0 was imposed, without airflow. Results are plotted in Figure 31.

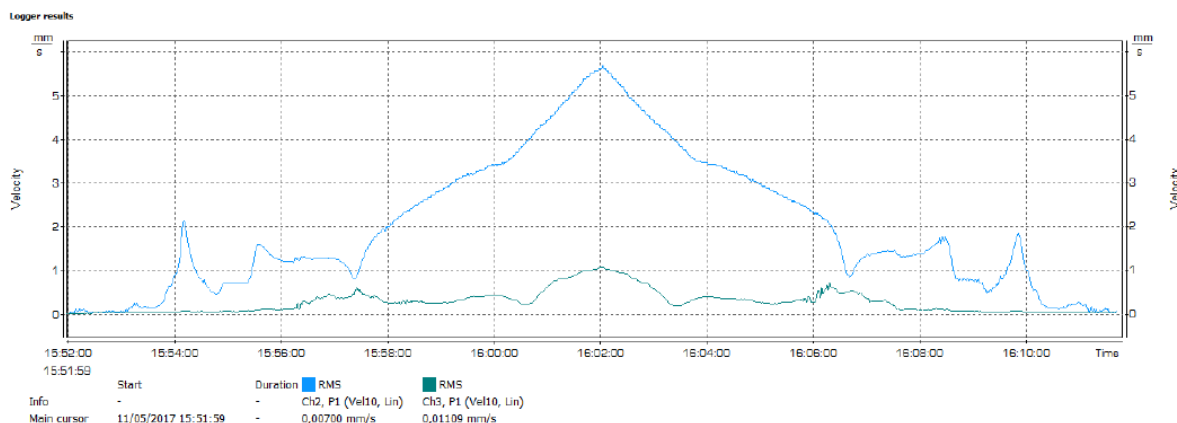


FIGURE 31: VIBRATION VELOCITY (RMS) AS A FUNCTION OF THE TURBINE ROTATION SPEED WITHOUT AIR FLOW.

4.6.1.2 TEST 1B: VIBRATION CONTROL IN THE RANGE OF ROTATION SPEEDS WITH AIRFLOW

The turbine is running using the generator as a motor. Rotation speed was set from 1,500 rpm to 2,500 rpm in steps of 250 rpm, with variable unidirectional airflow, from zero to full flow, period of variation from 3s to 10s, in steps of 1s, during 30 cycles. The largest RMS values of vibration velocities are shown in Table 5. Results of the vibration velocity for 2,500 rpm are plotted in Figure 32.

TABLE 5: MAXIMUM RMS VIBRATION VELOCITY FOR CONSTANT AS TURBINE ROTATION SPEED WITH VARIABLE AIR FLOW.

Test	Turbine rotation speed (rpm)	Maximum RMS vibration velocity (mm/s)
BA	2,500	6.3
BB	2,250	5.0
BC	2,000	3.7
BD	1,750	3.1
BE	1,500	2.3

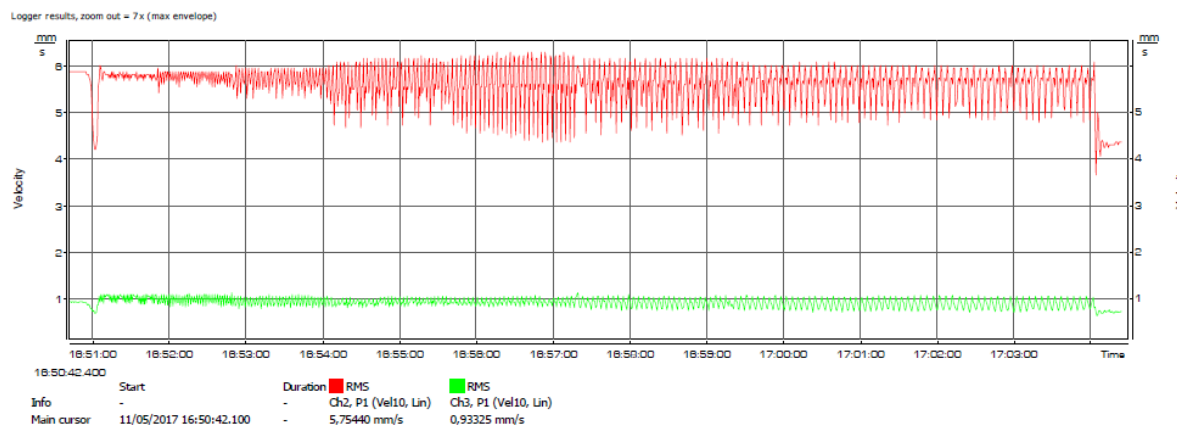


FIGURE 32: VIBRATION VELOCITY (RMS) FOR THE TURBINE OPERATING AT 2500 RPM WITH AIR FLOW.

4.6.2 HIGH-SPEED SAFETY-VALVE

4.6.2.1 HIGH-SPEED SAFETY-VALVE PRE-ASSEMBLY TESTS

Prior to the installation into the turbine, the HSSV was fully tested at Kymaner premises in February 2017. The tests objectives were:

- 1) Test for fatigue at a length time equivalent to the operation as a latching valve in Mutriku and evaluate effects;
- 2) Establish automatic procedure (code) to deal with single or multiple actuator malfunctions (test for fault in 1, 2 and 3);
- 3) Analyse behaviour of valve shutter in case of blockage at mid stroke and determine troubleshooting procedure;
- 4) Measure stroke speed and actuator force.

Results of the above tests are reported in APPENDIX A2.



FIGURE 33: HIGH-SPEED STOP-VALVE TESTING PRIOR TO TURBINE INSTALLATION.

4.6.2.2 HIGH-SPEED STOP-VALVE TESTS AFTER TURBINE INTEGRATION

The HSSV test on completion aimed at checking the valve behaviour under air flow after it has been installed in the turbine to allow comparison of the results with those of the preliminary test performed in February 2017.

Valve behaviour under normal operation

To analyse the valve behaviour under normal operation the following sequence of operations were performed:

- 1) set full flow on the blower;
- 2) impose 5 cycles of valve opening and closing (6 s open, 6 closed), and
- 3) measure current required per actuator.

Results of the above tests are reported in APPENDIX A3.

Valve behaviour under actuator failure

The behaviour of the valve was also analysed under single actuator failure and under two actuators failure. The following sequence of operations was performed:

- 4) 1) set full flow on the blower;
- 5) 2) generate the actuator failure condition;
- 6) 3) impose 5 cycles of valve opening and closing (4 s open, 2 closed)
- 7) 4) set turbine rotation speed to 1499 rpm, and
- 8) 5) measure current required per actuator.

Results of the above actuator failure tests are also reported in APPENDIX A3.

Valve behavior under air passage blockage

The valve was also tested under air passage blockage. The following sequence of operations was performed:

- 1) blower and turbine were turned off;
- 2) valve shutter was manually blocked with a wooden object preventing full closure;
- 3) actuator signals were recorded.

The contingency operation was identified and tested: valve opened and tried to close several times. Upon removal of the obstruction, the system was reset and the valve resumed normal operation.

Valve cyclic loading

The behaviour of the valve was analysed under cyclic loading. The following sequence of operations was performed:

- 1) set full flow on the blower;
- 2) set turbine rotation speed to 2,000 rpm;
- 3) impose open and close operations cycles during two hours (period 1s);
- 4) check system integrity and
- 5) measure temperature of actuators and current required per actuator.

Results of the cyclic loading tests are reported in APPENDIX A3.



5. CONCLUSIONS

Main conclusions of the testing are presented below:

- ▶ Results from the biradial turbine dry tests showed that the experimental values for the efficiency are fairly close to those predicted by the CFD calculations, thus validating the turbine design method.
- ▶ Electrical generator efficiency tests showed that very high efficiency is achieved in a wide range of rotation speeds and power, but a sharp drop of efficiency is observed for low power and low rotation speed. Furthermore, it is observed that the efficiency of the electrical generator decreases significantly for rotation speeds above 2,300 rpm.
- ▶ Several torque laws were implemented when testing the turbine in variable Gaussian flow. Results confirmed the effectiveness of changing the torque coefficients in constraining maximum speed and maximum allowed power.
- ▶ A HSSV valve safety control algorithm was implemented in order to shave power peaks under extreme wave conditions. Results showed that an aggressive valve control strategy successfully reduced any power peaks. This condition allowed the continuous operation of the turbine, even under excessively energetic wave climates.
- ▶ Turbine mechanical integrity tests were performed in different operating conditions. No vibration problems were identified that might lead to an early turbine failure.
- ▶ The high-speed safety valve was also fully tested to measure stroke speed and actuator forces in different operational conditions and to establish automatic procedure to deal with actuator malfunctions.

6. REFERENCES

Carrelhas, A. (2017). *Model testing of a biradial turbine*. Lisbon: IST Internal report.

Falcao, A., & Gato, L. (2012). Air turbines. In A. Sayigh, *Comprehensive Renewable Energy, Vol.8, Ocean Energy* (pp. 111-149). Oxford: Elsevier.



APPENDIX A1: TURBINE VIBRATION TESTS

This appendix presents the results of vibration levels under working conditions of the biradial turbine according ISO 14694:2003. This report has been requested by KYMANER.



RELATÓRIO

Cliente LABRV:	Kymaner - Tecnologias Energéticas, Lda. Estrada Paço do Lumiar, Campus do Lumiar Edif. D R/C, Sala 1026, Lisboa
Medição:	Turbina de Ar Biradial – projeto OPERA Medição de Vibrações Instituto Superior Técnico – Lisboa 2017
Dados:	OBRA N°: 17.00016.dbw.0018 RELATÓRIO REF°: LABRV/00723/17 TOTAL DE PÁGINAS: 16(relatório base + anexo I) e Anexo Certificado de Calibração ELABORADO POR: Carlos Aroeira Técnico do Laboratório de Ruído e Vibrações DATA DE REALIZAÇÃO DAS MEDIÇÕES: 12 de maio de 2017 DATA DE EMISSÃO DE RELATÓRIO: 13 de maio de 2017 NOTA: É expressamente proibida a reprodução parcial deste relatório sem autorização expressa do Laboratório. As conclusões apresentadas circunscrevem-se a situações idênticas à verificada à data dos ensaios.

ÍNDICE

1	INTRODUÇÃO	3
2	DESCRIÇÃO DO ENSAIO	3
2.1	Documentos de referência.....	3
2.2	Procedimento de medida	3
2.3	Calibração do equipamento.....	4
2.4	Condição de funcionamento da turbina durante as medidas	4
3	RESULTADOS DAS MEDIDAS	5
4	INTERPRETAÇÃO DOS RESULTADOS.....	5
4.1	Critério de avaliação.....	5
4.2	Avaliação dos resultados	6
5	CONCLUSÃO.....	6
	Anexo I – Resultados das Medidas	7
	Anexo II – Certificado de calibração	16

1 INTRODUÇÃO

Nome da empresa: Kymaner - Tecnologias Energéticas, Lda.

Local de ensaio: Instituto Superior Técnico – Lisboa

Ensaio efetuado: Medição de vibrações em turbina de ar

Objetivo do ensaio: Este estudo visou a determinação dos níveis de vibrações geradas em diversas condições de funcionamento de uma turbina e a sua avaliação de acordo com o definido na norma ISO 14694:2003.

2 DESCRIÇÃO DO ENSAIO

2.1 Documentos de referência

ISO 14694:2003 Industrial fans -- Specifications for balance quality and vibration levels

2.2 Procedimento de medida

Equipamento de medida: Medidor de vibrações de quatro canais SV948 ns 6995, acelerómetro triaxial PCB 356A15 ns 139283

Calibrador de vibrações IMI M394C06 SN 5936

Montagem do acelerómetro: na flange do motor elétrico, com base magnética, conforme se pode ver nas fotografias



Eixo 1 e 2: direções radiais
Eixo 3: direção vertical

Parâmetros de medida: Velocidade RMS, espectro de frequência

Gama de frequência de medida: 10 Hz 5 KHz

Periodicidade de registo: uma vez por segundo

2.3 Calibração do equipamento

Verificação da cadeia de medida: antes do início do ensaio a cadeia de medida foi verificada com o calibrador de vibrações.

Calibração do equipamento: em anexo encontra-se certificado de calibração

2.4 Condição de funcionamento da turbina durante as medidas

Foram realizadas medidas na máquina, montada numa estrutura provisória, nas condições de funcionamento que se listadas na tabela a seguir apresentada.

Referência do Ensaio	Condição de funcionamento da máquina
1.A	Variação de velocidade durante o arranque até se atingir a velocidade máxima seguido de paragem, sem caudal de ar
1.BA	Velocidade constante (2500 RPM) e caudal de ar variável
1.BB	Velocidade constante (2250 RPM) e caudal de ar variável
1.BC	Velocidade constante (2000 RPM) e caudal de ar variável
1.BD	Velocidade constante (1750 RPM) e caudal de ar variável
1.BE	Velocidade constante (1500 RPM) e caudal de ar variável

3 RESULTADOS DAS MEDIDAS

No Anexo I encontram-se os gráficos com os resultados das medidas.

Os maiores dos valores de velocidade de vibração rms, obtidos em cada condição de funcionamento da máquina, foram os que se podem ver na tabela a seguir apresentada.

Referência do Ensaio	Condição de funcionamento da máquina	Máximo da Velocidade RMS (mm/s)
1.A	Variação de velocidade, sem caudal de ar	5,6
1.BA	Velocidade constante (2500 RPM) e caudal de ar variável	6,3
1.BB	Velocidade constante (2250 RPM) e caudal de ar variável	5,0
1.BC	Velocidade constante (2000 RPM) e caudal de ar variável	3,7
1.BD	Velocidade constante (1750 RPM) e caudal de ar variável	3,1
1.BE	Velocidade constante (1500 RPM) e caudal de ar variável	2,3

4 INTERPRETAÇÃO DOS RESULTADOS

4.1 Critério de avaliação

De acordo com a informação fornecida a máquina testada é da categoria BV-3.

De acordo com a ISO 14694:2003 têm-se o limite de acordo com a tabela a seguir apresentada.

Tipo de limite	Valor de vibração em mm/s rms
Limite de vibração para um ensaio in-situ, para uma máquina da classe BV-3, no arranque, em base flexível	6,3

4.2 Avaliação dos resultados

A estrutura provisória onde a máquina se encontrava instalada durante o ensaio não permite que o ensaio realizado seja classificado como um ensaio in-situ.

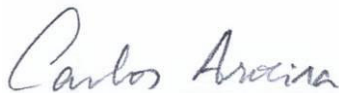
Também tem de se considerar não estar garantido que a estrutura provisória de apoio da máquina não tenha frequências naturais na gama de velocidades de rotação da máquina durante o ensaio.

Assim os resultados das medidas não podem ser avaliados à luz do definido na norma ISO 14694:2003.

5 CONCLUSÃO

Os resultados das medidas não podem ser avaliados à luz do definido na norma ISO 14694:2003 não sendo assim a avaliação do ensaio conclusiva.

Elaborado por:

A handwritten signature in black ink that reads 'Carlos Aroeira'.

Carlos Aroeira

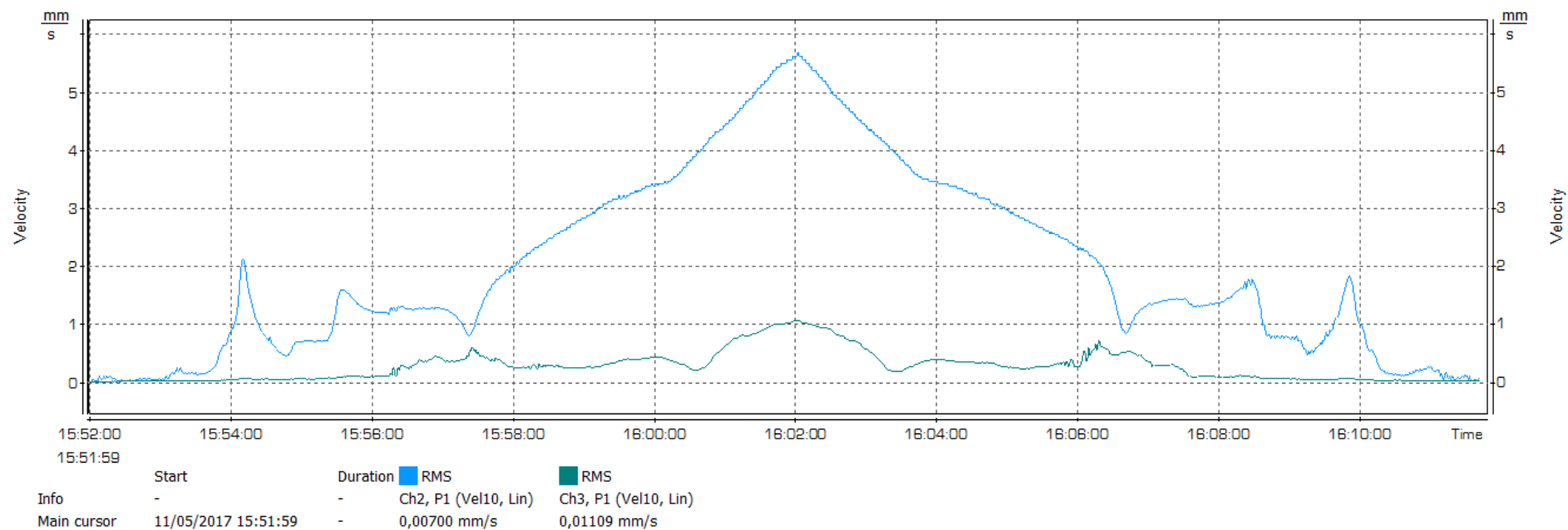
Técnico do Laboratório de Ruído e Vibrações

Anexo I – Resultados das Medidas

Ensaio 1.A Variação de velocidade sem caudal de ar

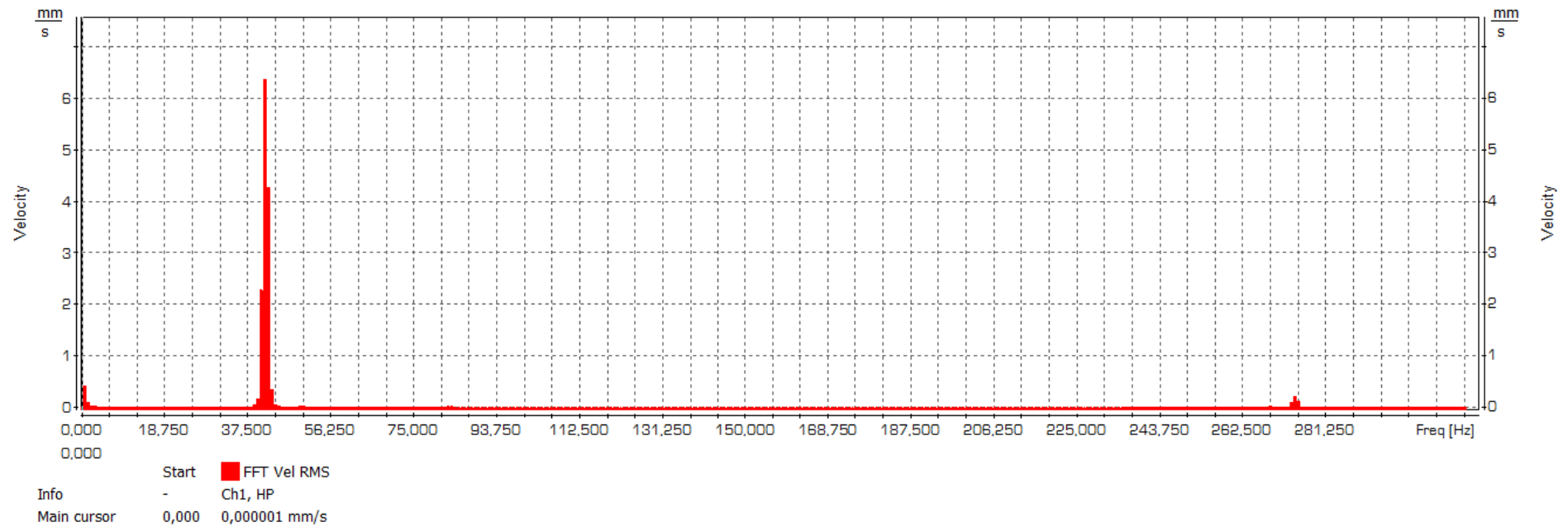
Evolução da velocidade RMS

Logger results

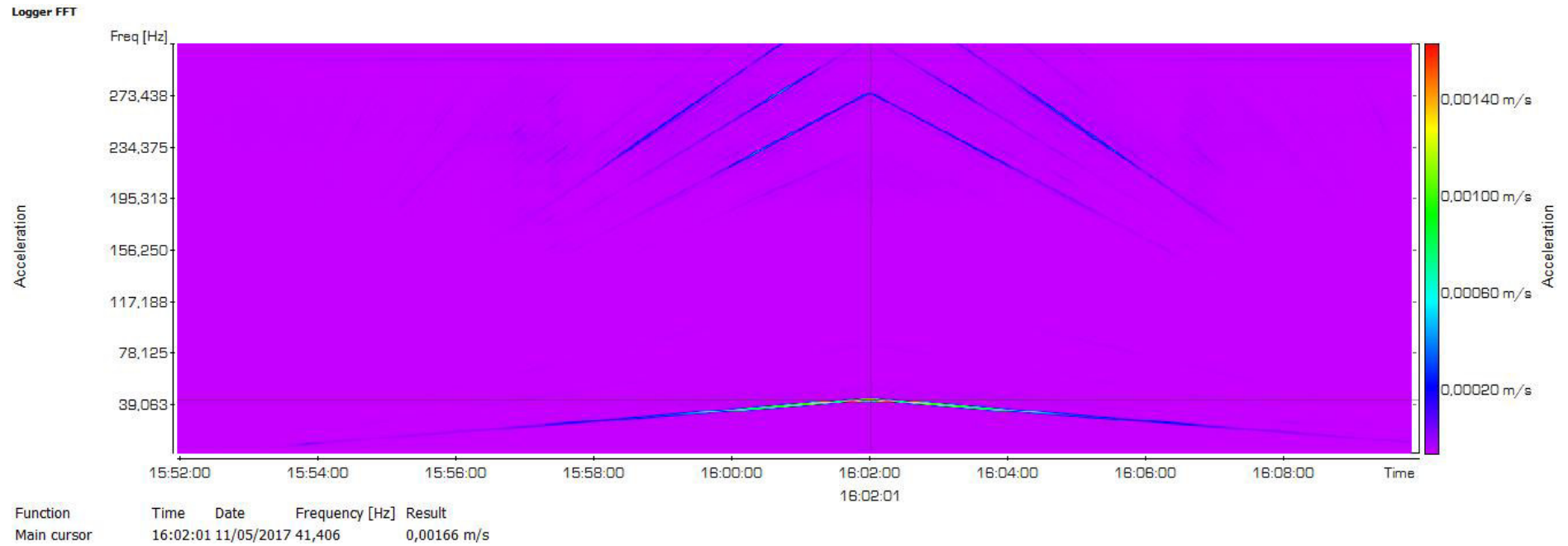


Espectro de frequência à velocidade máxima

Logger FFT, 11/05/2017 16:01:59



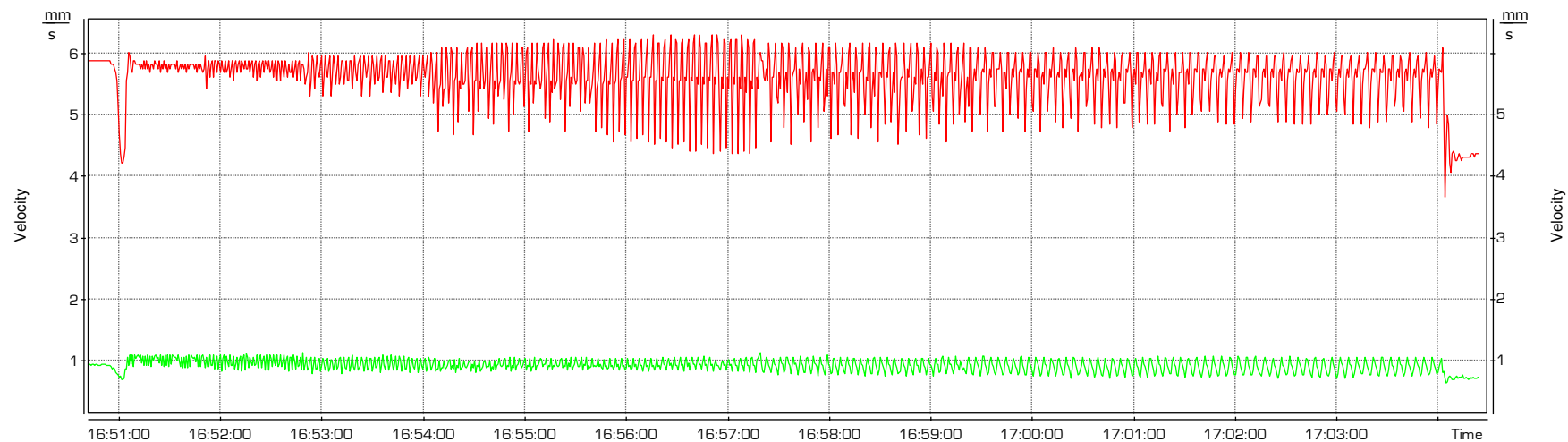
Evolução do espectro de frequência durante o ensaio



Ensaio 1.BA Velocidade constante (2500 RPM) e caudal de ar variável

Evolução da velocidade RMS

Logger results, zoom out = 7x (max envelope)

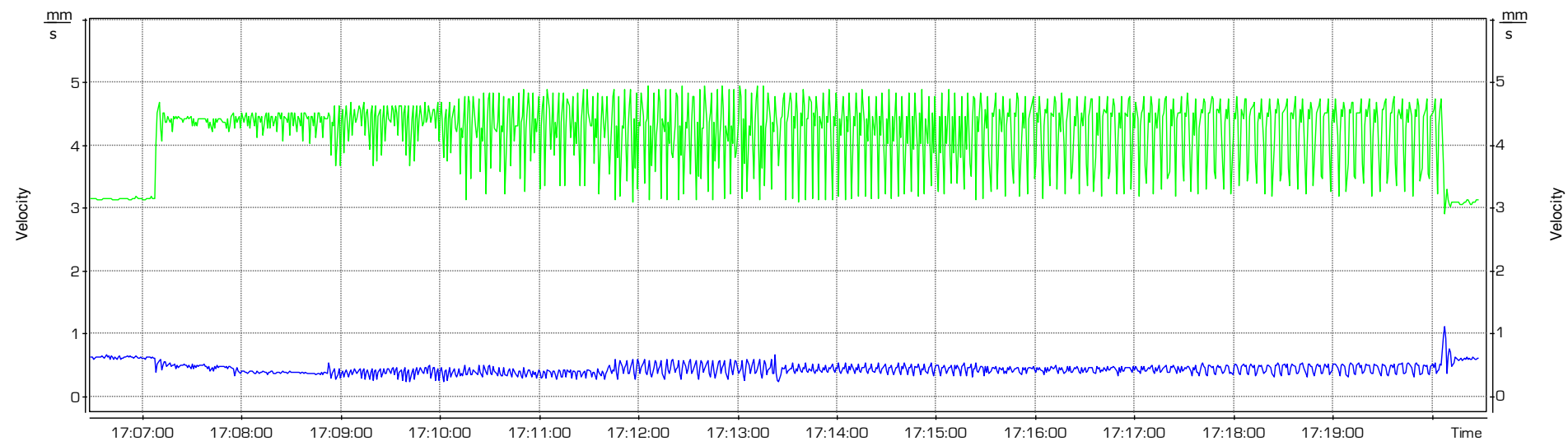


Info	Start	Duration	Ch2, P1 (Vel10, Lin)	Ch3, P1 (Vel10, Lin)
Main cursor	11/05/2017 16:50:42.100	-	5,75440 mm/s	0,93325 mm/s

Ensaio 1.BB Velocidade constante (2250 RPM) e caudal de ar variável

Evolução da velocidade RMS

Logger results, zoom out = 8x (max envelope)



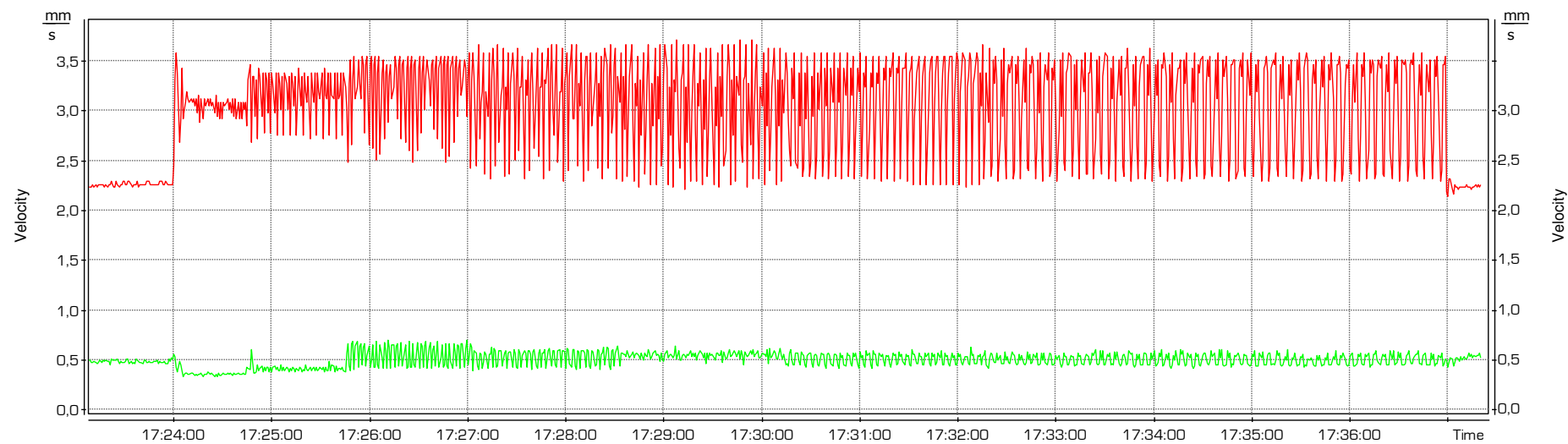
17:06:28.100

	Start	Duration	■ RMS	■ RMS
Info	-	-	Ch2, P1 (Vel10, Lin)	Ch3, P1 (Vel10, Lin)
Main cursor	11/05/2017 17:06:28.100	-	max:3,16228 mm/s	max:0,62373 mm/s

Ensaio 1.BC Velocidade constante (2000 RPM) e caudal de ar variável

Evolução da velocidade RMS

Logger results, zoom out = 8x (max envelope)



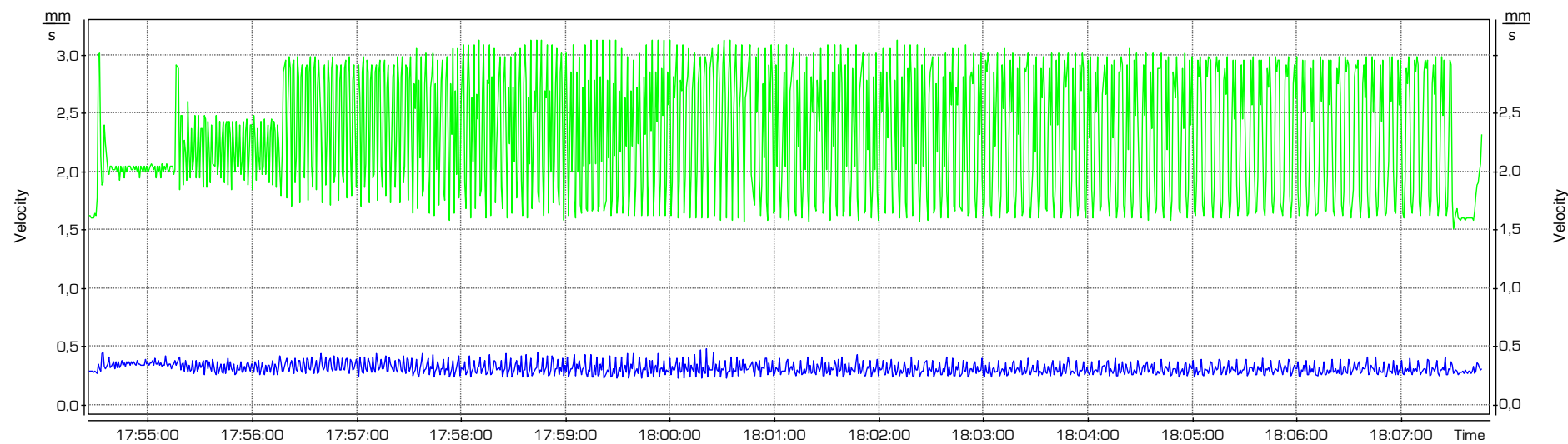
17:23:08.200

	Start	Duration	■ RMS	■ RMS
Info	-	-	Ch2, P1 (Vel10, Lin)	Ch3, P1 (Vel10, Lin)
Main cursor	11/05/2017 17:23:08.100	-	2,16272 mm/s	0,43652 mm/s

I
Ensaio 1.BD Velocidade constante (1750 RPM) e caudal de ar variável

Evolução da velocidade RMS

Logger results, zoom out = 7x (max envelope)

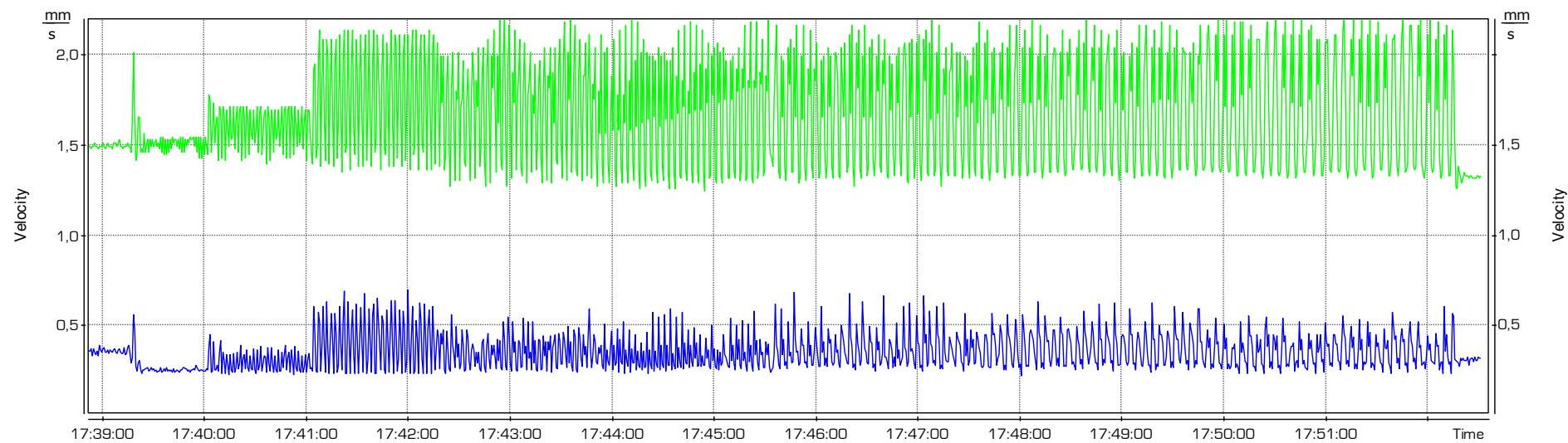


17:54:26.700	Start	Duration	■ RMS	■ RMS
Info	-	-	Ch2, P1 (Vel10, Lin)	Ch3, P1 (Vel10, Lin)
Main cursor	11/05/2017 17:54:26.700	-	max:1,62181 mm/s	max:0,28840 mm/s

Ensaio 1.BE Velocidade constante (1500 RPM) e caudal de ar variável

Evolução da velocidade RMS

Logger results, zoom out = 7x (max envelope)



17:38:52.100	Start	Duration	■ RMS	■ RMS
Info	-	-	Ch2, P1 (Vel10, Lin)	Ch3, P1 (Vel10, Lin)
Main cursor	11/05/2017 17:38:52.100	-	1,49624 mm/s	0,34277 mm/s

Anexo II – Certificado de calibração



Instalações
de Oeiras

Signature Not
Verified

Digitally signed by
LABMETRO ONLINE
Date: 2016.12.23
15:08:55 +00:00
Reason: Documento
aprovado
electronicamente



IPAC
acreditação

M0059
Calibração

Laboratório de Calibração em
Metrologia Electro-Física

Certificado de calibração

Data de emissão

2016-12-22

Serviço nº. CACV1321/16

Página 1 de 14

Equipamento

SISTEMA DE MEDIÇÃO DE VIBRAÇÃO CORPO HUMANO

Unidade de Leitura

Marca: SVANTEK
Modelo: SVAN 948
Nº série: 6985
Nº ident.: **LR105**

Acelerómetro Triaxial - Mão-Braço

Marca: DYTRAN Nº série: **9516**
Modelo: 3023M2 Nº ident.: ---

Assento Triaxial - Corpo Inteiro

Marca: SVANTEK Nº série: **842S**
Modelo: SV 39A Nº ident.: ---
Aceler.: Dytran - 3143M1 Nº série: **842**

Cliente

dBWave.I Acoustic Engineering, S.A.

Rua do Mirante, 258, Parque Industrial de Grijó
4415-491 Grijó VNG

Data de
Calibração

2016-12-22

Condições
Ambientais

Temperatura: 23,0 °C Humidade relativa: 52,0 %hr Pressão atmosférica: 101,1 kPa

Procedimento

PO.M-DM/VIB 01 (Ed. C - Rev. 01).

Rastreabilidade

Sensibilidade de Vibração, Acelerómetro padrão PCB 301A11, rastreado a Spektra (Alemanha).

Tensão alternada, Fluke 5790A, Fluke A40/A40A rastreado à 1A CAL, Kassel (Alemanha, Dakks).

Tempo e Frequência, Hewlett Packard 58503A, rastreado ao Tempo Universal Coordenado (UTC) pelo sinal difundido pelo Global Positioning System (GPS).

Estado do
equipamento

Não foram identificados aspectos relevantes que afectassem os resultados.

Resultados

Encontram-se apresentados na(s) página(s) seguinte(s).

"A incerteza expandida apresentada está expressa pela incerteza-padrão multiplicada pelo factor de expansão $k=2$, o qual para uma distribuição normal corresponde a uma probabilidade de 95%, aproximadamente. A incerteza foi calculada de acordo com o documento EA-4/02."

Calibrado por

João Pedro Martins

Responsável pela Validação

Luís Ferreira (Responsável Técnico)



IPAC
accreditação

M0059
Calibração

Laboratório de Calibração em
Metrologia Electro-Física

Certificado de calibração

nº. CACV1321/16

Página 2 de 14

Inscrições no equipamento e informação documentada

REQUISITOS

Referência para a norma que é aplicável	ISO 8041:2005
Indicação do fabricante do equipamento	CONFORME
Indicação do modelo do equipamento	CONFORME
Indicação do número de série do equipamento	CONFORME
Documentação referente às diversas partes do equipamento	CONFORME
Referência às especificações em unidades SI	CONFORME
Documentação referente às funcionalidades do equipamento	CONFORME
Informação geral	CONFORME
Funcionalidades	CONFORME
Sensibilidade de vibração	CONFORME
Sensibilidade à variação das condições ambientais	CONFORME
Fonte de alimentação	CONFORME
Transductor de vibração	CONFORME
Acessórios	CONFORME
Utilização do equipamento	CONFORME
Informação adicional para teste	CONFORME
Informação suplementar	CONFORME

Calibrado por

João Pedro Martins

Responsável pela Validação

Luís Ferreira (Responsável Técnico)



IPAC
accreditação

M0059
Calibração

Laboratório de Calibração em
Metrologia Electro-Física

Certificado de calibração

nº. CACV1321/16

Página 3 de 14

Funcionalidades imperativas e genéricas

REQUISITOS - Características gerais

Apresenta o valor de medição de aceleração ponderada em média no tempo	CONFORME
Apresenta o valor de medição de aceleração em limitação de banda em média no tempo	CONFORME
Apresenta o valor de duração da medição	CONFORME
Apresenta indicação de sobrecarga em qualquer altura da medição	CONFORME
Permite o ajuste de sensibilidade de vibração	CONFORME
Referência às gamas de medição e qual a gama de referência	CONFORME
Referência ao uso da função "hold"	CONFORME
Referência à possibilidade de substituição do transdutor por sinal eléctrico	CONFORME
Referência ao valor máximo que poderá ser aplicado nos testes eléctricos	CONFORME

REQUISITOS - Linearidade em amplitude

Gama de linearidade de referência maior do que 60 dB	CONFORME
Referência à gama de linearidade de valores com erros de linearidade inferior a 6%	CONFORME
Sobreposição de gamas de medição superior a 40 dB	CONFORME
Referência ao limite inferior e superior de medição de cada gama	CONFORME

REQUISITOS - Indicação do parâmetro de medição

Identificação inequívoca do parâmetro de medição	CONFORME
Descrição no manual dos diversos parâmetros de medição	CONFORME
Indicação da ponderação em frequência do parâmetro a analisar	CONFORME
Indicação dos factores multiplicativos usados na medição em combinação de eixos	CONFORME
Referência hardware e métodos usados para a transferência de dados por comunicação	CONFORME
Indicação do valor medido com resolução inferior a 1%	CONFORME
Tempo apropriado de actualização do ecrã	CONFORME
Referência aos diversos tempos de actualização de ecrã disponíveis	CONFORME
Tempo de estabilização e "warm up" inferior a 2 minutos	CONFORME
Indicação de pronto a usar	CONFORME
Tempo de actuação de início de medição inferior a 0,5 segundos	CONFORME
Indicação inequívoca de inicialização ou de medição em progresso	CONFORME
Referência às características de saída eléctrica de sinal, quando aplicável	CONFORME

Referência ao tipo de baterias a usar no equipamento	CONFORME
Existência de filtro de limitação de banda	CONFORME

Calibrado por

João Pedro Martins

Responsável pela Validação

Luís Ferreira (Responsável Técnico)



Laboratório de Calibração em
Metrologia Electro-Física

Certificado de calibração

nº. CACV1321/16

Página 4 de 14

TESTES MECÂNICOS

Indicação à frequência de referência sobre condições de referência

Determinação da sensibilidade de vibração do transductor, à frequência de referência

SISTEMA MÃO-BRAÇO

Frequência	Canal / Eixo de medição	Sensibilidade	Sensibilidade	Incerteza expandida
159,2 Hz	Canal 1 / X	1,091 mV/m/s ²	10,70 mV/g	± 1,2 %
	Canal 2 / Y	0,993 mV/m/s ²	9,74 mV/g	± 1,2 %
	Canal 3 / Z	1,076 mV/m/s ²	10,55 mV/g	± 1,2 %

SISTEMA CORPO INTEIRO

Frequência	Canal / Eixo de medição	Sensibilidade	Sensibilidade	Incerteza expandida
159,2 Hz	Canal 1 / X	9,83 mV/m/s ²	96,4 mV/g	± 1,2 %
	Canal 2 / Y	9,95 mV/m/s ²	97,5 mV/g	± 1,2 %
	Canal 3 / Z	9,67 mV/m/s ²	94,8 mV/g	± 1,2 %
15,92 Hz	Canal 1 / X	10,00 mV/m/s ²	98,0 mV/g	± 1,2 %
	Canal 2 / Y	10,13 mV/m/s ²	99,3 mV/g	± 1,2 %
	Canal 3 / Z	9,84 mV/m/s ²	96,5 mV/g	± 1,2 %

Calibrado por

João Pedro Martins

Responsável pela Validação

Luís Ferreira (Responsável Técnico)



IPAC
accreditação

M0059
Calibração

Laboratório de Calibração em
Metrologia Electro-Física

Certificado de calibração

nº. CACV1321/16

Página 5 de 14

Cadeia de medição

W_h - malha de ponderação mão-braço

Frequência analisada	Amplitude de referência	Valor de referência	Valor do equipamento	Erro	Incerteza expandida	Especificação da norma	Resultado
19,95 Hz	10 m/s ²	7,82 m/s ²	7,68 m/s ²	-1,8 %	± 3 %	+12%, -11%	OK
39,81 Hz	10 m/s ²	4,11 m/s ²	4,06 m/s ²	-1,2 %	± 3 %	+12%, -11%	OK
79,43 Hz	10 m/s ²	2,02 m/s ²	2,01 m/s ²	-0,5 %	± 3 %	+12%, -11%	OK
100,00 Hz	10 m/s ²	1,60 m/s ²	1,59 m/s ²	-0,6 %	± 3 %	+12%, -11%	OK
158,49 Hz	10 m/s ²	1,007 m/s ²	0,99 m/s ²	-1,7 %	± 3 %	+12%, -11%	OK
316,23 Hz	10 m/s ²	0,503 m/s ²	0,499 m/s ²	-0,8 %	± 3 %	+12%, -11%	OK
398,11 Hz	10 m/s ²	0,398 m/s ²	0,394 m/s ²	-1,0 %	± 3 %	+12%, -11%	OK
630,96 Hz	10 m/s ²	0,245 m/s ²	0,243 m/s ²	-0,8 %	± 3 %	+12%, -11%	OK
1000,00 Hz	10 m/s ²	0,135 m/s ²	0,138 m/s ²	2,2 %	± 3 %	+26%, -21%	OK

W_a - malha de ponderação corpo inteiro

Frequência analisada	Amplitude de referência	Valor de referência	Valor do equipamento	Erro	Incerteza expandida	Especificação da norma	Resultado
15,85 Hz	10 m/s ²	1,27 m/s ²	1,26 m/s ²	-0,8 %	± 3 %	+12%, -11%	OK
39,81 Hz	10 m/s ²	0,500 m/s ²	0,493 m/s ²	-1,4 %	± 3 %	+12%, -11%	OK
79,43 Hz	10 m/s ²	0,210 m/s ²	0,209 m/s ²	-0,5 %	± 3 %	+26%, -21%	OK
100,00 Hz	10 m/s ²	0,140 m/s ²	0,139 m/s ²	-0,7 %	± 3 %	+26%, -21%	OK

Ruído interno

W_h - malha de ponderação mão-braço

Valor de ruído determinado 0,023 m/s²

W_k - malha de ponderação corpo inteiro

Valor de ruído determinado 0,002 m/s²

Calibrado por

João Pedro Martins

Responsável pela Validação

Luís Ferreira (Responsável Técnico)



Laboratório de Calibração em
Metrologia Electro-Física

Certificado de calibração

nº. CACV1321/16

Página 6 de 14

TESTES ELÉTRICOS

Indicação à frequência de referência sobre condições de referência

Malha	Frequência de referência	Amplitude de referência	Valor de referência	Valor do equipamento	Erro	Incerteza expandida	Especificação da norma	Erro % Especificação
Wh	79,58 Hz	10 m/s ²	2,020 m/s ²	2,020 m/s ²	0,00 %	± 2 %	± 4 %	± 0 %
Wd	15,92 Hz	1 m/s ²	0,126 m/s ²	0,126 m/s ²	0,00 %	± 2 %	± 4 %	± 0 %
Wk	15,92 Hz	1 m/s ²	0,772 m/s ²	0,772 m/s ²	-0,06 %	± 2 %	± 4 %	± 2 %

Cross-talk

Valor de referência	Canal em teste	Valor do equipamento	Diferença encontrada	Especificação da norma	Resultado
Canal 1 238 m/s ²	Canal 2	0,03 m/s ²	0,01 %	< 0,5 %	OK
	Canal 3	0,02 m/s ²	0,01 %	< 0,5 %	OK
Canal 2 238 m/s ²	Canal 1	0,03 m/s ²	0,01 %	< 0,5 %	OK
	Canal 3	0,02 m/s ²	0,01 %	< 0,5 %	OK
Canal 3 238 m/s ²	Canal 1	0,02 m/s ²	0,01 %	< 0,5 %	OK
	Canal 2	0,02 m/s ²	0,01 %	< 0,5 %	OK

Calibrado por

João Pedro Martins

Responsável pela Validação

Luís Ferreira (Responsável Técnico)



IPAC
acreditação

M0059
Calibração

Laboratório de Calibração em
Metrologia Electro-Física

Certificado de calibração

nº. CACV1321/16

Página 7 de 14

Linearidade em amplitude e indicação a baixo da gama

Frequência analisada	Valor de referência	Valor do equipamento	Erro	Incerteza expandida	Especificação da norma	Erro % Especificação
8 Hz	110 dB	110,3 dB	3,5 %	± 2 %	± 6 %	59 %
	111 dB	111,3 dB	3,5 %	± 2 %	± 6 %	59 %
	112 dB	112,2 dB	2,3 %	± 2 %	± 6 %	39 %
	113 dB	113,2 dB	2,3 %	± 2 %	± 6 %	39 %
	114 dB	114,1 dB	1,2 %	± 2 %	± 6 %	19 %
	115 dB	115,1 dB	1,2 %	± 2 %	± 6 %	19 %
	120 dB	120,0 dB	0,0 %	± 2 %	± 6 %	0 %
	125 dB	125,0 dB	0,0 %	± 2 %	± 6 %	0 %
	130 dB	130,0 dB	0,0 %	± 2 %	± 6 %	0 %
	135 dB	135,0 dB	0,0 %	± 2 %	± 6 %	0 %
	140 dB	140,0 dB	0,0 %	± 2 %	± 6 %	0 %
	145 dB	145,0 dB	0,0 %	± 2 %	± 6 %	0 %
	150 dB	150,0 dB	0,0 %	± 2 %	± 6 %	0 %
	155 dB	155,0 dB	0,0 %	± 2 %	± 6 %	0 %
	160 dB	160,0 dB	0,0 %	± 2 %	± 6 %	0 %
	165 dB	165,0 dB	0,0 %	± 2 %	± 6 %	0 %
	170 dB	170,0 dB	0,0 %	± 2 %	± 6 %	0 %
	175 dB	175,0 dB	0,0 %	± 2 %	± 6 %	0 %
	180 dB	180,0 dB	0,0 %	± 2 %	± 6 %	0 %
	185 dB	185,0 dB	0,0 %	± 2 %	± 6 %	0 %
	190 dB	190,0 dB	0,0 %	± 2 %	± 6 %	0 %
	195 dB	195,0 dB	0,0 %	± 2 %	± 6 %	0 %
	196 dB	196,0 dB	0,0 %	± 2 %	± 6 %	0 %
	197 dB	197,0 dB	0,0 %	± 2 %	± 6 %	0 %
	198 dB	198,0 dB	0,0 %	± 2 %	± 6 %	0 %
	197 dB	197,0 dB	0,0 %	± 2 %	± 6 %	0 %
	196 dB	196,0 dB	0,0 %	± 2 %	± 6 %	0 %
	195 dB	195,0 dB	0,0 %	± 2 %	± 6 %	0 %
	190 dB	190,0 dB	0,0 %	± 2 %	± 6 %	0 %
	185 dB	185,0 dB	0,0 %	± 2 %	± 6 %	0 %
	180 dB	180,0 dB	0,0 %	± 2 %	± 6 %	0 %
	175 dB	175,0 dB	0,0 %	± 2 %	± 6 %	0 %
	170 dB	170,0 dB	0,0 %	± 2 %	± 6 %	0 %
	165 dB	165,0 dB	0,0 %	± 2 %	± 6 %	0 %
	160 dB	160,0 dB	0,0 %	± 2 %	± 6 %	0 %

Calibrado por

João Pedro Martins

Responsável pela Validação

Luís Ferreira (Responsável Técnico)



IPAC
acreditação

M0059
Calibração

Laboratório de Calibração em
Metrologia Electro-Física

Certificado de calibração

nº. CACV1321/16

Página 8 de 14

Linearidade em amplitude e indicação a baixo da gama (Cont.)

Frequência analisada	Valor de referência	Valor do equipamento	Erro	Incerteza expandida	Especificação da norma	Erro % Especificação
8 Hz	155 dB	155,0 dB	0,0 %	± 2 %	± 6 %	0 %
	150 dB	150,0 dB	0,0 %	± 2 %	± 6 %	0 %
	145 dB	145,0 dB	0,0 %	± 2 %	± 6 %	0 %
	140 dB	140,0 dB	0,0 %	± 2 %	± 6 %	0 %
	135 dB	135,0 dB	0,0 %	± 2 %	± 6 %	0 %
	130 dB	130,0 dB	0,0 %	± 2 %	± 6 %	0 %
	125 dB	125,0 dB	0,0 %	± 2 %	± 6 %	0 %
	120 dB	120,0 dB	0,0 %	± 2 %	± 6 %	0 %
	115 dB	115,1 dB	1,2 %	± 2 %	± 6 %	19 %
	114 dB	114,1 dB	1,2 %	± 2 %	± 6 %	19 %
	113 dB	113,2 dB	2,3 %	± 2 %	± 6 %	39 %
112 dB	112,2 dB	2,3 %	± 2 %	± 6 %	39 %	
111 dB	111,3 dB	3,5 %	± 2 %	± 6 %	59 %	
110 dB	110,3 dB	3,5 %	± 2 %	± 6 %	59 %	
80 Hz	110 dB	110,3 dB	3,5 %	± 2 %	± 6 %	59 %
	111 dB	111,3 dB	3,5 %	± 2 %	± 6 %	59 %
	112 dB	112,3 dB	3,5 %	± 2 %	± 6 %	59 %
	113 dB	113,2 dB	2,3 %	± 2 %	± 6 %	39 %
	114 dB	114,1 dB	1,2 %	± 2 %	± 6 %	19 %
	115 dB	115,1 dB	1,2 %	± 2 %	± 6 %	19 %
	120 dB	120,0 dB	0,0 %	± 2 %	± 6 %	0 %
	125 dB	125,0 dB	0,0 %	± 2 %	± 6 %	0 %
	130 dB	130,0 dB	0,0 %	± 2 %	± 6 %	0 %
	135 dB	135,0 dB	0,0 %	± 2 %	± 6 %	0 %
	140 dB	140,0 dB	0,0 %	± 2 %	± 6 %	0 %
	145 dB	145,0 dB	0,0 %	± 2 %	± 6 %	0 %
	150 dB	150,0 dB	0,0 %	± 2 %	± 6 %	0 %
	155 dB	155,0 dB	0,0 %	± 2 %	± 6 %	0 %
	160 dB	160,0 dB	0,0 %	± 2 %	± 6 %	0 %
	165 dB	165,0 dB	0,0 %	± 2 %	± 6 %	0 %
	170 dB	170,0 dB	0,0 %	± 2 %	± 6 %	0 %
175 dB	175,0 dB	0,0 %	± 2 %	± 6 %	0 %	
180 dB	180,0 dB	0,0 %	± 2 %	± 6 %	0 %	
185 dB	185,0 dB	0,0 %	± 2 %	± 6 %	0 %	

Calibrado por

João Pedro Martins

Responsável pela Validação

Luís Ferreira (Responsável Técnico)

O IPAC é signatário do Acordo de Reconhecimento Mútuo da EA e do ILAC para ensaios, calibrações e inspeções. IPAC is a signatory to the EA MLA and ILAC MRA for testing, calibration and inspection. Este documento só pode ser reproduzido na íntegra, excepto quando autorização por escrito do ISQ. This document may not be reproduced other than in full, except with the prior written approval of the issuing laboratory.

DM/064.2/07



IPAC
acreditação

M0059
Calibração

Laboratório de Calibração em
Metrologia Electro-Física

Certificado de calibração

nº. CACV1321/16

Página 9 de 14

Linearidade em amplitude e indicação a baixo da gama (Cont.)

Frequência analisada	Valor de referência	Valor do equipamento	Erro	Incerteza expandida	Especificação da norma	Erro % Especificação
80 Hz	190 dB	190,0 dB	0,0 %	± 2 %	± 6 %	0 %
	195 dB	195,0 dB	0,0 %	± 2 %	± 6 %	0 %
	196 dB	196,0 dB	0,0 %	± 2 %	± 6 %	0 %
	197 dB	197,0 dB	0,0 %	± 2 %	± 6 %	0 %
	198 dB	198,0 dB	0,0 %	± 2 %	± 6 %	0 %
	197 dB	197,0 dB	0,0 %	± 2 %	± 6 %	0 %
	196 dB	196,0 dB	0,0 %	± 2 %	± 6 %	0 %
	195 dB	195,0 dB	0,0 %	± 2 %	± 6 %	0 %
	190 dB	190,0 dB	0,0 %	± 2 %	± 6 %	0 %
	185 dB	185,0 dB	0,0 %	± 2 %	± 6 %	0 %
	180 dB	180,0 dB	0,0 %	± 2 %	± 6 %	0 %
	175 dB	175,0 dB	0,0 %	± 2 %	± 6 %	0 %
	170 dB	170,0 dB	0,0 %	± 2 %	± 6 %	0 %
	165 dB	165,0 dB	0,0 %	± 2 %	± 6 %	0 %
	160 dB	160,0 dB	0,0 %	± 2 %	± 6 %	0 %
	155 dB	155,0 dB	0,0 %	± 2 %	± 6 %	0 %
	150 dB	150,0 dB	0,0 %	± 2 %	± 6 %	0 %
	145 dB	145,0 dB	0,0 %	± 2 %	± 6 %	0 %
	140 dB	140,0 dB	0,0 %	± 2 %	± 6 %	0 %
	135 dB	135,0 dB	0,0 %	± 2 %	± 6 %	0 %
130 dB	130,0 dB	0,0 %	± 2 %	± 6 %	0 %	
125 dB	125,0 dB	0,0 %	± 2 %	± 6 %	0 %	
120 dB	120,0 dB	0,0 %	± 2 %	± 6 %	0 %	
115 dB	115,1 dB	1,2 %	± 2 %	± 6 %	19 %	
114 dB	114,2 dB	2,3 %	± 2 %	± 6 %	39 %	
113 dB	113,2 dB	2,6 %	± 2 %	± 6 %	43 %	
112 dB	112,3 dB	3,5 %	± 2 %	± 6 %	59 %	
111 dB	111,3 dB	3,5 %	± 2 %	± 6 %	59 %	
110 dB	110,3 dB	3,5 %	± 2 %	± 6 %	59 %	
800 Hz	110 dB	110,3 dB	3,5 %	± 2 %	± 6 %	59 %
	111 dB	111,2 dB	2,3 %	± 2 %	± 6 %	39 %
	112 dB	112,2 dB	2,3 %	± 2 %	± 6 %	39 %
	113 dB	113,1 dB	1,2 %	± 2 %	± 6 %	19 %
	114 dB	114,0 dB	0,0 %	± 2 %	± 6 %	0 %

Calibrado por

João Pedro Martins

Responsável pela Validação

Luís Ferreira (Responsável Técnico)



IPAC
acreditação

M0059
Calibração

Laboratório de Calibração em
Metrologia Electro-Física

Certificado de calibração

nº. CACV1321/16

Página 10 de 14

Linearidade em amplitude e indicação a baixo da gama (Cont.)

Frequência analisada	Valor de referência	Valor do equipamento	Erro	Incerteza expandida	Especificação da norma	Erro % Especificação
800 Hz	115 dB	115,0 dB	0,0 %	± 2 %	± 6 %	0 %
	120 dB	120,0 dB	0,0 %	± 2 %	± 6 %	0 %
	125 dB	125,0 dB	0,0 %	± 2 %	± 6 %	0 %
	130 dB	130,0 dB	0,0 %	± 2 %	± 6 %	0 %
	135 dB	135,0 dB	0,0 %	± 2 %	± 6 %	0 %
	140 dB	140,0 dB	0,0 %	± 2 %	± 6 %	0 %
	145 dB	145,0 dB	0,0 %	± 2 %	± 6 %	0 %
	150 dB	150,0 dB	0,0 %	± 2 %	± 6 %	0 %
	155 dB	155,0 dB	0,0 %	± 2 %	± 6 %	0 %
	160 dB	160,0 dB	0,0 %	± 2 %	± 6 %	0 %
	165 dB	165,0 dB	0,0 %	± 2 %	± 6 %	0 %
	170 dB	170,0 dB	0,0 %	± 2 %	± 6 %	0 %
	175 dB	175,0 dB	0,0 %	± 2 %	± 6 %	0 %
	180 dB	180,0 dB	0,0 %	± 2 %	± 6 %	0 %
	185 dB	185,0 dB	0,0 %	± 2 %	± 6 %	0 %
	190 dB	190,0 dB	0,0 %	± 2 %	± 6 %	0 %
	195 dB	195,0 dB	0,0 %	± 2 %	± 6 %	0 %
	196 dB	196,0 dB	0,0 %	± 2 %	± 6 %	0 %
	197 dB	197,0 dB	0,0 %	± 2 %	± 6 %	0 %
	198 dB	198,0 dB	0,0 %	± 2 %	± 6 %	0 %
	197 dB	197,0 dB	0,0 %	± 2 %	± 6 %	0 %
	196 dB	196,0 dB	0,0 %	± 2 %	± 6 %	0 %
	195 dB	195,0 dB	0,0 %	± 2 %	± 6 %	0 %
	190 dB	190,0 dB	0,0 %	± 2 %	± 6 %	0 %
	185 dB	185,0 dB	0,0 %	± 2 %	± 6 %	0 %
	180 dB	180,0 dB	0,0 %	± 2 %	± 6 %	0 %
	175 dB	175,0 dB	0,0 %	± 2 %	± 6 %	0 %
	170 dB	170,0 dB	0,0 %	± 2 %	± 6 %	0 %
	165 dB	165,0 dB	0,0 %	± 2 %	± 6 %	0 %
	160 dB	160,0 dB	0,0 %	± 2 %	± 6 %	0 %
	155 dB	155,0 dB	0,0 %	± 2 %	± 6 %	0 %
	150 dB	150,0 dB	0,0 %	± 2 %	± 6 %	0 %
	145 dB	145,0 dB	0,0 %	± 2 %	± 6 %	0 %
	140 dB	140,0 dB	0,0 %	± 2 %	± 6 %	0 %
	135 dB	135,0 dB	0,0 %	± 2 %	± 6 %	0 %

Calibrado por

João Pedro Martins

Responsável pela Validação

Luís Ferreira (Responsável Técnico)



Laboratório de Calibração em
Metrologia Electro-Física

Certificado de calibração

nº. CACV1321/16

Página 11 de 14

Linearidade em amplitude e indicação a baixo da gama (Cont.)

Frequência analisada	Valor de referência	Valor do equipamento	Erro	Incerteza expandida	Especificação da norma	Erro % Especificação
800 Hz	130 dB	130,0 dB	0,0 %	± 2 %	± 6 %	0 %
	125 dB	125,0 dB	0,0 %	± 2 %	± 6 %	0 %
	120 dB	120,0 dB	0,0 %	± 2 %	± 6 %	0 %
	115 dB	115,0 dB	0,0 %	± 2 %	± 6 %	0 %
	114 dB	114,0 dB	0,0 %	± 2 %	± 6 %	0 %
	113 dB	113,1 dB	1,2 %	± 2 %	± 6 %	19 %
	112 dB	112,1 dB	1,2 %	± 2 %	± 6 %	19 %
	111 dB	111,2 dB	2,3 %	± 2 %	± 6 %	39 %
	110 dB	110,3 dB	3,5 %	± 2 %	± 6 %	59 %

Calibrado por

João Pedro Martins

Responsável pela Validação

Luís Ferreira (Responsável Técnico)



IPAC
acreditação

M0059
Calibração

Laboratório de Calibração em
Metrologia Electro-Física

Certificado de calibração

nº. CACV1321/16

Página 12 de 14

Resposta em frequência

W_d - malha de ponderação mão-brço

Frequência analisada	Valor de referência	Valor do equipamento	Erro	Incerteza expandida	Especificação da norma	Resultado
3,98 Hz	2,03 m/s ²	2,02 m/s ²	-0,5 %	± 3 %	+26%, -100%	OK
5,01 Hz	2,04 m/s ²	2,02 m/s ²	-1,0 %	± 3 %	+26%, -21%	OK
6,31 Hz	2,04 m/s ²	2,02 m/s ²	-1,0 %	± 3 %	+26%, -21%	OK
7,94 Hz	2,04 m/s ²	2,02 m/s ²	-1,0 %	± 3 %	+26%, -21%	OK
10,00 Hz	2,03 m/s ²	2,02 m/s ²	-0,5 %	± 3 %	+12%, -11%	OK
12,59 Hz	2,04 m/s ²	2,02 m/s ²	-1,0 %	± 3 %	+12%, -11%	OK
15,85 Hz	2,02 m/s ²	2,02 m/s ²	0,0 %	± 3 %	+12%, -11%	OK
19,95 Hz	2,04 m/s ²	2,02 m/s ²	-1,0 %	± 3 %	+12%, -11%	OK
25,12 Hz	2,05 m/s ²	2,02 m/s ²	-1,5 %	± 3 %	+12%, -11%	OK
31,62 Hz	2,02 m/s ²	2,02 m/s ²	0,0 %	± 3 %	+12%, -11%	OK
39,81 Hz	2,02 m/s ²	2,02 m/s ²	0,0 %	± 3 %	+12%, -11%	OK
50,12 Hz	2,02 m/s ²	2,02 m/s ²	0,0 %	± 3 %	+12%, -11%	OK
63,10 Hz	2,02 m/s ²	2,02 m/s ²	0,0 %	± 3 %	+12%, -11%	OK
79,43 Hz	2,03 m/s ²	2,02 m/s ²	-0,4 %	± 3 %	+12%, -11%	OK
100,00 Hz	2,02 m/s ²	2,02 m/s ²	0,1 %	± 3 %	+12%, -11%	OK
125,89 Hz	2,04 m/s ²	2,02 m/s ²	-1,0 %	± 3 %	+12%, -11%	OK
158,49 Hz	2,02 m/s ²	2,02 m/s ²	0,0 %	± 3 %	+12%, -11%	OK
199,53 Hz	2,05 m/s ²	2,02 m/s ²	-1,5 %	± 3 %	+12%, -11%	OK
251,19 Hz	2,02 m/s ²	2,02 m/s ²	0,0 %	± 3 %	+12%, -11%	OK
316,23 Hz	2,04 m/s ²	2,02 m/s ²	-1,0 %	± 3 %	+12%, -11%	OK
398,11 Hz	2,06 m/s ²	2,02 m/s ²	-2,0 %	± 3 %	+12%, -11%	OK
501,19 Hz	2,06 m/s ²	2,02 m/s ²	-2,0 %	± 3 %	+12%, -11%	OK
630,96 Hz	2,06 m/s ²	2,02 m/s ²	-2,0 %	± 3 %	+12%, -11%	OK
794,33 Hz	2,03 m/s ²	2,02 m/s ²	-0,5 %	± 3 %	+12%, -11%	OK
1000,00 Hz	2,02 m/s ²	2,02 m/s ²	0,0 %	± 3 %	+26%, -21%	OK
1258,93 Hz	1,97 m/s ²	2,02 m/s ²	2,4 %	± 3 %	+26%, -21%	OK

Calibrado por

João Pedro Martins

Responsável pela Validação

Luís Ferreira (Responsável Técnico)



IPAC
accreditação

M0059
Calibração

Laboratório de Calibração em
Metrologia Electro-Física

Certificado de calibração

nº. CACV1321/16

Página 13 de 14

Resposta em frequência

W_d - malha de ponderação corpo inteiro

Frequência analisada	Valor de referência	Valor do equipamento	Erro	Incerteza expandida	Especificação da norma	Resultado
0,50 Hz	1,28 m/s ²	1,26 m/s ²	-1,5 %	± 3 %	+26%, -21%	OK
0,63 Hz	1,27 m/s ²	1,26 m/s ²	-0,7 %	± 3 %	+12%, -11%	OK
0,79 Hz	1,27 m/s ²	1,26 m/s ²	-0,8 %	± 3 %	+12%, -11%	OK
1,00 Hz	1,29 m/s ²	1,26 m/s ²	-2,4 %	± 3 %	+12%, -11%	OK
2,00 Hz	1,27 m/s ²	1,26 m/s ²	-0,7 %	± 3 %	+12%, -11%	OK
5,01 Hz	1,26 m/s ²	1,26 m/s ²	-0,2 %	± 3 %	+12%, -11%	OK
15,85 Hz	1,26 m/s ²	1,26 m/s ²	-0,1 %	± 3 %	+12%, -11%	OK
39,81 Hz	1,27 m/s ²	1,26 m/s ²	-0,8 %	± 3 %	+12%, -11%	OK
79,43 Hz	1,28 m/s ²	1,26 m/s ²	-1,4 %	± 3 %	+26%, -21%	OK
100,00 Hz	1,27 m/s ²	1,26 m/s ²	-1,0 %	± 3 %	+26%, -21%	OK

W_k - malha de ponderação corpo inteiro

Frequência analisada	Valor de referência	Valor do equipamento	Erro	Incerteza expandida	Especificação da norma	Resultado
0,50 Hz	7,88 m/s ²	7,77 m/s ²	-1,4 %	± 3 %	+26%, -21%	OK
0,63 Hz	7,89 m/s ²	7,77 m/s ²	-1,5 %	± 3 %	+12%, -11%	OK
0,79 Hz	7,83 m/s ²	7,77 m/s ²	-0,7 %	± 3 %	+12%, -11%	OK
1,00 Hz	7,87 m/s ²	7,77 m/s ²	-1,3 %	± 3 %	+12%, -11%	OK
2,00 Hz	7,84 m/s ²	7,77 m/s ²	-0,9 %	± 3 %	+12%, -11%	OK
5,01 Hz	7,81 m/s ²	7,77 m/s ²	-0,5 %	± 3 %	+12%, -11%	OK
15,85 Hz	7,77 m/s ²	7,77 m/s ²	-0,1 %	± 3 %	+12%, -11%	OK
39,81 Hz	7,81 m/s ²	7,77 m/s ²	-0,5 %	± 3 %	+12%, -11%	OK
79,43 Hz	7,82 m/s ²	7,77 m/s ²	-0,6 %	± 3 %	+26%, -21%	OK
100,00 Hz	7,81 m/s ²	7,77 m/s ²	-0,5 %	± 3 %	+26%, -21%	OK

Calibrado por

João Pedro Martins

Responsável pela Validação

Luís Ferreira (Responsável Técnico)

O IPAC é signatário do Acordo de Reconhecimento Mútuo da EA e do ILAC para ensaios, calibrações e inspeções. IPAC is a signatory to the EA MLA and ILAC MRA for testing, calibration and inspection. Este documento só pode ser reproduzido na íntegra, excepto quando autorização por escrito do ISQ. This document may not be reproduced other than in full, except with the prior written approval of the issuing laboratory.

DM/064.2/07



Laboratório de Calibração em
Metrologia Electro-Física

Certificado de calibração

nº. CACV1321/16

Página 14 de 14

Indicação de sobrecarga

Sinal aplicado	Indicação de sobrecarga	Diferença entre medições	Incerteza expandida	Especificação da norma	Erro % Especificação
Pulsos positivos	4070 m/s ²	0,2 %	± 2 %	± 15 %	1 %
Pulsos negativos	4060 m/s ²				

Medição combinada entre eixos

W_h - malha de ponderação mão-braço

Sinal aplicado	Amplitude de referência	Valor de referência	Valor do equipamento	Valor total calculado	Valor total lido no equip.	Erro	Incerteza expandida	Especificação da norma	Erro % Especificação
Canal 1	10 m/s ²	2,024 m/s ²	2,02 m/s ²	3,50 m/s ²	3,5 m/s ²	0,0 %	± 1 %	± 3 %	0 %
Canal 2	10 m/s ²	2,024 m/s ²	2,02 m/s ²						
Canal 3	10 m/s ²	2,024 m/s ²	2,02 m/s ²						

Calibrado por

João Pedro Martins

Responsável pela Validação

Luís Ferreira (Responsável Técnico)

O IPAC é signatário do Acordo de Reconhecimento Mútuo da EA e do ILAC para ensaios, calibrações e inspeções. IPAC is a signatory to the EA MLA and ILAC MRA for testing, calibration and inspection. Este documento só pode ser reproduzido na íntegra, excepto quando autorização por escrito do ISQ. This document may not be reproduced other than in full, except with the prior written approval of the issuing laboratory.

DM/064.2/07

APPENDIX A2: HSSV PRELIMINARY TESTS

This appendix presents the results of the HSSV testing at Kymaner premises in February 2017.



Open Sea Operating Experience To Reduce Wave Energy Costs



This project has received funding from the European Union's Horizon 2020
Research and innovation programme under grant agreement No 654444



B	Revisão geral	01-02-2017	N. Brinquete	J.Varandas			J.Varandas
A	Alterações onde indicado com letra (A)	07-12-2016	N. Brinquete	J.Varandas			J.Varandas
Índice	Revisão	Data	Elaborado	Verificado	Verificado		Aprovado
Index	Modification	Date	Prepared by	Checked T	Checked P		Approved

L.Peças/Partslist	WA No
Dimensão/Dimension	Classe/Class Ne
Grupo/Group	Tipo/Type

TÍTULO/TITLE	Escala/Scale
High Speed Stop Valve preliminary test	
PTO Assembly	
	Peso/Weight (kg)
	Material

LTU	Data/Date	Nome/Name	Cliente/Cient	OPERA H2020	
Elaborado/Prepared by	15-06-2016	N. Brinquete	Escalão/Plant		
Verificado/Checked T			Projecto/Project Ne	KO34.2016	
Verificado/Checked P	15-06-2016	J.Varandas	Contrato/Contract Ne	654444	Similar
Aprovado/Approved	15-06-2016	J.Varandas	Arquivo/File		Substitui/Replace

	N.º interno/Internal no.	+		
		=		
	Documento n.º/Document no.	Índice/Index	F/Sht	1
	OPE-100-PT-0007	B	De/Of	7

TÍTULO/TITLE
High Speed Stop Valve preliminary test

1) GENERAL CHARACTERISTICS

Equipment:	High Speed Stop Valve
Project Name:	OPERA H2020
Reference Drawings:	OPE-103-DE-0105-01 OPE-103-DE-0104-01
Actuator supplier:	Festo
Test Duration	1 month
Year of production:	2016
Valve type	Cylindrical
Shutter material	Low friction (PE or aluminium)
Valve operating system	Linear actuators
Number of actuators	4
Voltage	230V AC
Actuator housing	Inside nacelle
Protection Index of actuators	IP 65
Environmental conditions shutter	100% relative humidity with salt particles
Environmental conditions actuators	Dry with possibility of salt water vapour in vicinity
Operating temperature	TBD
Latching operation mode (MUTRIKU)	
Operating time	60 days
Acting speed	0,3 m/s
Period of operation	4 s
Safety Operation Mode (BIMEP)	
Operating time	2 years
Acting speed	6 cm/s
Period of operation	1 day

2) TEST OBJECTIVES

- 1 – Test for fatigue at a length of time equivalent to the operation as a latching valve in Mutriku and evaluate effects
- 2 – Establish automatic procedure (code) to deal with single or multiple actuator malfunctions (test for fault in 1, 2 and 3)
- 3 – Analyse behaviour of valve shutter in case of blockage at mid stroke and determine troubleshooting procedure (A)
(c.f. §3.2 Technical Specification)
- 4 – Measure stroke speed and actuator force

3) INSTALLATION / MATERIAL REQUIREMENTS

- Test rig where to install the HSSV subassembly;
- HSSV subassembly ready for installation in the PTO;
- Actuators, drivers and PC for movement control
- Control SW and operating manuals of actuators
- Power supply
- Current meter
- Reference Drawings (OPE-103-DE-0105-01; OPE-103-DE-0104-01)
- Signal collector (Data Acquisition interface)

<input checked="" type="checkbox"/>

	Documento n.º/Document no.	Índice/Index	FI/Sht	2
	OPE-100-PT-0007	B	De/Of	7

TÍTULO/TITLE
High Speed Stop Valve preliminary test

4) TEST PROCEDURE

a) Install actuators and cabling

b) Test electrical connections

Power supply

Actuator movement (4 in synch, opposite pairs, 1 by one)

4 in synch

opposite pair 1

opposite pair 2

actuator 1

actuator 2

actuator 3

actuator 4

Position indication

actuator 1

actuator 2

actuator 3

actuator 4

Current measurement

actuator 1

actuator 2

actuator 3

actuator 4

[A]	2,6
[A]	2,6
[A]	2,2
[A]	2,4

c) Connect shutter to the actuators

d) Program actuator stroke (0-56mm) and operating speed for 0.3m/s and period at 4s

e) Test rig has been assembled and HSSV is ready to operate (acc to Ref. Drwg OPE-103-DE-0105-01)

Executed by

NUNO BRINQUETE 

Date:

15 / 2 / 2017

Aproved by (Kymaner)

JOSÉ VARANDAS 

Date:

15 / 2 / 2017

Validated by (IST)

JOÃO HENRIQUES 

Date:

15 / 2 / 2017



Documento n.º/Document no.

OPE-100-PT-0007

Índice/Index

B

Ft/Sht

3

De/Of

7

TÍTULO/TITLE
High Speed Stop Valve preliminary test

f) Test movement of shutter and record reference values

Current measurement

- actuator 1
- actuator 2
- actuator 3
- actuator 4

[A]	2,6
[A]	2,6
[A]	2,2
[A]	2,2

g) Keep Open/Close operation cycles running for 1 hour and check

- Stability of installation (T=1s)
- Temperature of actuators (max °C)

37,2

h) Keep Open/Close operation cycles running for 6 hours and check

- Stability of installation (T=1s)
- Temperature of actuators (max °C)

37,3

i) Keep Open/Close operation cycles running for 24 hours and check

- Stability of installation (T=1s)
- Temperature of actuators (max °C)
- Record reference values

37,8

Current measurement

- actuator 1
- actuator 2
- actuator 3
- actuator 4

[A]	2,6
[A]	2,6
[A]	2,2
[A]	2,2

Executed by

NUNO BRINQUETE

Date:

15 / 2 / 2017

Aproved by (Kymaner)

JOSÉ VARANDAS

Date:

15 / 2 / 2017

Validated by (IST)

JOÃO HENRIQUES

Date:

15 / 2 / 2017



Documento n.º/Document no.

OPE-100-PT-0007

Índice/Index

B

Ft/Sht

4

De/Of

7

TÍTULO/TITLE

High Speed Stop Valve preliminary test

j) Keep Open/Close operation cycles running for 48 hours and check

Stability of installation (T=1s)

Temperature of actuators (max °C)

Record reference values

Current measurement

actuator 1

actuator 2

actuator 3

actuator 4

37,8

[A]	2,6
[A]	2,6
[A]	2,2
[A]	2,2

5) Establish procedure to deal with valve shutter jamming at mid-stroke

l) Identify actuator by fault signal

Record reference values

Current measurement

actuator 1

actuator 2

actuator 3

actuator 4

[A]	3,4
[A]	3,4
[A]	1,4
[A]	1,4

m) Program actuator drivers for response to jamming and check behaviour.

NOTE: the following sequence has to be confirmed and adapted during the test

- 1 - Drivers must reverse the movement
- 2 - Drivers to repeat the movement
- 3 - Repeat sequence 3 times and assume close position in case of failure to close
- 4 - Remove object preventing movement and resume operation

Executed by

NUNO BRINQUETE

NB

Date:

15 / 2 / 2017

Approved by (Kymaner)

JOSÉ VARANDAS

JV

Date:

15 / 2 / 2017

Validated by (IST)

JOÃO HENRIQUES

JH

Date:

15 / 2 / 2017



Documento n.º/Document no.

OPE-100-PT-0007

Índice/Index

B

Fi/Sht

5

De/Of

7

TÍTULO/TITLE
High Speed Stop Valve preliminary test

6) Establish procedure to deal with actuators failure

A) Failure of 1 actuator

- n) Identify faulty actuator and release brake
Operate alternative pair of actuators and control end positions
actuators 1-3
actuators 2-4

Program actuator drivers for response to actuator fault and check behaviour.

	<input checked="" type="checkbox"/>
opened	closed
<input checked="" type="checkbox"/>	<input checked="" type="checkbox"/>
<input checked="" type="checkbox"/>	<input checked="" type="checkbox"/>
	<input checked="" type="checkbox"/>

B) Failure of 2 actuators

- o) Identify faulty actuators and release brake

Operate alternative pair of actuators and control end positions
actuators 1-3
actuators 1-2
actuators 3-4

Program actuator drivers for response to 2 actuators fault and check behaviour.

	<input checked="" type="checkbox"/>
opened	closed
<input checked="" type="checkbox"/>	<input checked="" type="checkbox"/>
<input type="checkbox"/>	<input type="checkbox"/>
<input type="checkbox"/>	<input type="checkbox"/>
	<input checked="" type="checkbox"/>

*NOP
NOP*

Executed by NUNO BRINQUETE *NPB*
 Aproved by (Kymaner) JOSÉ VARANDAS *JV*
 Validated by (IST) JOÃO HENRIQUES *JH*

Date: 15 / 2 / 2017
 Date: 15 / 2 / 2017
 Date: 15 / 2 / 2017



Documento n.º/Document no.
OPE-100-PT-0007

B	Fi/Sht	6
	De/Of	7

TÍTULO/TITLE
High Speed Stop Valve preliminary test

C) Failure of 3 actuators

- m) Identify faulty actuators and release brakes
 Operate remaining actuators and control end positions
 - actuator 1
 - actuator 2
 - actuator 3
 - actuator 4

	<input checked="" type="checkbox"/>	
opened	closed	
<input type="checkbox"/>	<input type="checkbox"/>	NOP
<input type="checkbox"/>	<input type="checkbox"/>	NOP
<input type="checkbox"/>	<input type="checkbox"/>	NOP
<input type="checkbox"/>	<input type="checkbox"/>	NOP
	<input type="checkbox"/>	NOP

Program actuator drivers for response to actuator fault and check behaviour.

CONCLUSION: the HSSV is validated as fit to operate and begin the tests after integration in the turbine.

jo

Executed by NUNO BRINQUETE *RB*
 Approved by (Kymaner) JOSÉ VARANDAS *jo*
 Validated by (IST) JOÃO HENRIQUES *JH*

Date: 15 / 2 / 2017
 Date: 15 / 2 / 2017
 Date: 15 / 2 / 2017

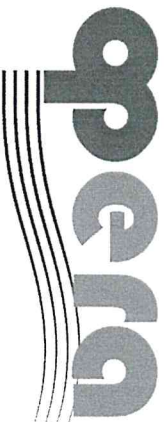
	Documento n.º/Document no. OPE-100-PT-0007	Indice/Index	7
		B Fl/Sht De/Of	7

APPENDIX A3: MECHANICAL INTEGRITY TESTS

This appendix presents the results of the mechanical integrity tests and HSSV behaviour under normal operation, actuator failure and cyclic loading.



Open Sea Operating
Experience To Reduce Wave
Energy Costs



This project has received funding from the European Union's Horizon 2020
Research and innovation programme under grant agreement No 654444



EVE | Ente Vasco
de la Energía



B	Tests 1A and 1B plots	09/05/2017	N. Brinquete	J.Varandas	-	J.Varandas			
A	revised according to TD "Minimum dry lab tests required to novel PTO" (Oceanic) 04/05/2017	08/06/2017	N. Brinquete	J.Varandas	-	J.Varandas			
-	original version	15/06/2016	N. Brinquete	J.Varandas	-	J.Varandas			
Índice	Revisão	Data	Elaborado	Verificado	Verificado	Verificado	Preparado by	Checked T	Checked P
Índice	Modification	Date	Prepared by	Checked T	Checked P	Approved			

L.Pecas/Partelist

MA No

Dimensão/Dimension

Class/Class No

Grupo/Group

Tipo/Type

TÍTULO/TITLE

Escala/Scale

Dry Lab Tests of PTO mechanical integrity + HSSV TOC

Peso/Weight (kg)

Material

PTO Assembly

LTU	Data/Date	Nome/Name	Cliente/Client	OPERA H2020		
Elaborado/Prepared by	15/06/2016	N. Brinquete	Escala/Plant			
Verificado/Checked T			Project/Project No	KO34.2016		
Verificado/Checked P	15/06/2016	J.Varandas	Contract/Contract No	654444	Similar	
Aprovado/Approved	15/06/2016	J.Varandas	Arquivo/File		Substitui/Replace	

N.º interno/Internal no.

+

Documento n.º Document no.

Índice/Index

OPE-100-PT-0008

B

F/Sht 1

De/Of 8



Dry Lab Tests of PTO mechanical integrity + HSSV TOC

1) GENERAL CHARACTERISTICS

Project Name:	OPERA H2020
Power Take Off unit	
Turbine:	Radial turbine
Reference Drawings:	OPE-100-DE-0102-01 OPE-103-DE-0104-01 SIEMENS 30kW SIEMENS 400V AC
Generator	
Power Electronics	
Aerodynamic test rig characteristics	
Blower power:	55 kW
Turbine-generator electrical power:	30 kW
Flow characteristics	Unidirectional variable flow by fan variable speed and high-speed control valve
Control	In loop pneumatic power
High Speed Stop/Safety Valve (HSSV)	
HSSV Actuator supplier:	Festo
Test Duration	1 week
Year of production:	2016
High Speed Valve type	Cylindrical
Shutter material	PEHD
Valve operating system	Linear actuators
Number of actuators	4
Voltage	230V AC

2) TEST OBJECTIVES

1- TURBINE TEST

The objective of the mechanical integrity tests is to identify any vibration problems which may lead to an early turbine failure in different operating conditions

2- High Speed Safety Valve test

The HSSV Tests on Completion (TOC) aim at checking the valve behaviour under air flow after it has been installed in the turbine and compare the results with those of the preliminary test (OPE-100-PT-0007) performed in February 2017

Analysing valve behaviour under 1 or 2 actuators failure
 Analyse behaviour under valve air passage blockage
 Analyse fatigue behaviour under cyclic loading

3) INSTALLATION / MATERIAL REQUIREMENTS

- Aerodynamic test rig with PTO installed ready to operate
- Operating PTO
- Operating HSSV
- Power electronics ready to operate
- All necessary sensors ready to operate (*)
- Data Acquisition system ready to operate

<input checked="" type="checkbox"/>					
-------------------------------------	-------------------------------------	-------------------------------------	-------------------------------------	-------------------------------------	-------------------------------------

() Accelerometers replaced with PC3356 A45 (test data collected by external company D3value)*



Documento n.º/Document no.

OPE-100-PT-0008

Índice/Index

B

Ft/Sht

2

Del/or

8

TITULO/TITLE

Dry Lab Tests of PTO mechanical integrity + HSSV TOC

Test 1A: Vibrations control in the full range of rotational speeds without airflow

Turbine is run using the generator as a motor.

- a) A ramp up from 0 rpm to 2500 rpm is imposed
Ramp time ~ 10 min

Output: RMS and peak acceleration vs turbine rotational speed

Acceleration

(See Annex)

rotational speed

- b) A ramp down from 2500 rpm to 0 rpm is imposed
Ramp time ~ 10 min

Output: RMS acceleration vs turbine rotational speed

Acceleration

(See Annex)

rotational speed

Executed by IST

Ana Carneiros

Date: 11 / 5 / 2017

Validated by Kymaner

José Vazquez

Date: 11 / 5 / 2017

Approved by Oceantec

Date: / /



Documento n.º/Document no.

OPE-100-PT-0008

Índice/Index

B

F/Sheet

3

D/Of

8

Dry Lab Tests of PTO mechanical integrity + HSSV TOC

Test 1B: Vibrations control in the full range of rotational speeds with airflow.

Turbine is run using the generator as a motor.

Rotational speed from 500 rpm to 2500 rpm (in steps of 250 rpm)

Period should change from 3s to 10s (in steps of 1 second)

Variable unidirectional airflow, from zero flow to full flow

Number of cycles, 30

Max air flow

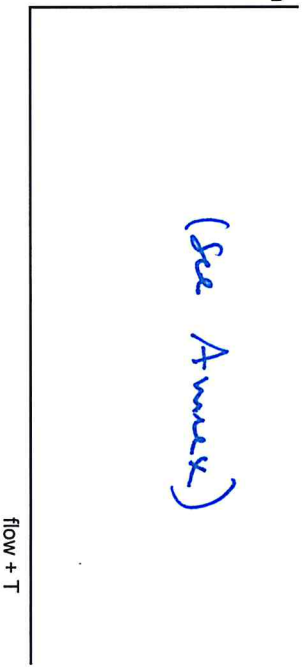
Output:

Turbine rpm, period, input flow and vibration RMS values

Speed (rpm)	750	1000	1250	1500	1750	2000	2250	2500
500	3 s	3 s	3 s	3 s	3 s	3 s	3 s	3 s
3 s	4 s	4 s	4 s	4 s	4 s	4 s	4 s	4 s
4 s	5 s	5 s	5 s	5 s	5 s	5 s	5 s	5 s
5 s	6 s	6 s	6 s	6 s	6 s	6 s	6 s	6 s
6 s	7 s	7 s	7 s	7 s	7 s	7 s	7 s	7 s
7 s	8 s	8 s	8 s	8 s	8 s	8 s	8 s	8 s
8 s	9 s	9 s	9 s	9 s	9 s	9 s	9 s	9 s
9 s	10 s	10 s	10 s	10 s	10 s	10 s	10 s	10 s

Speed (rpm)	X
Period	Y

(See Annex)



Executed by IST Ana Canvalho Date: 11 / 5 / 2017

Validated by Kymaner JOS VASUNDAS Date: 11 / 5 / 2017

Approved by Oceantec _____ Date: _____

Documento n.º/Document no. **OPÉ-100-PT-0008**

Índice/Index **B**

Ft/Shl	4
Del/Of.	8

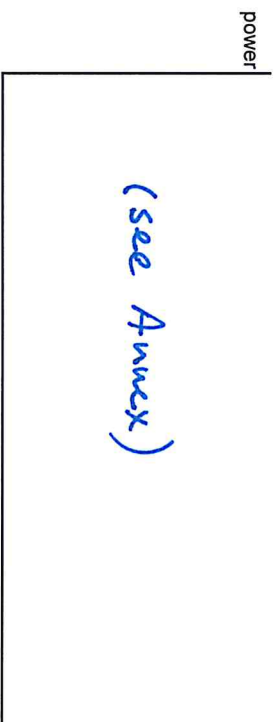
Dry Lab Tests of PTO mechanical integrity + HSSV TOC

Test 2A: Analyse valve behaviour under normal operation

1. Set full flow
2. Impose 5 cycles of valve opening and closings. ~~2s~~-open-~~4s~~-closed **6s - 75% Open**
3. Set turbine rotational speed to ~~2000 RPM~~ **1198 RPM**
Measure current required per actuator (máx)

	Open	Close
actuator 1	[A] 2,2	[A] 1,7
actuator 2	[A] 2,7	[A] 0,5
actuator 3	[A] 1,9	[A] 1,6
actuator 4	[A] 2,1	[A] 1,7

Plot the input power received in the turbine vs. time



Turn off the power electronics and check turbine runs down safely.

OK NOK

Test 2B: Analyse valve behaviour under single actuator failure

1. Set full air flow
2. Generate a failure condition in one of the actuators
3. Impose 5 cycles of valve opening and closings ~~As~~ open - ~~2s~~ closed
4. Set turbine rotational speed to **2000 RPM 1499**

Actuator nr 1

	Open	Close
actuator 1	[A] —	[A] —
actuator 2	[A] 1,1	[A] 1,0
actuator 3	[A] —	[A] —
actuator 4	[A] 2,4	[A] 0,7

Plot the input power received in the turbine vs. time (i.e. 2A)

Turn off the power electronics and check turbine runs down safely.

OK NOK

Executed by IST

Ana Carvalho

Date: 11 / 5 / 2017

Validated by Kymaner

Fosé VAREZAS

Date: 11 / 5 / 2017

Approved by Oceantec

Date: / /



Documento n.º/Document no.

OPe-100-PT-0008

Índice/Index

B

F/Sheet 5

De/Of 8

Dry Lab Tests of PTO mechanical integrity + HSSV TOC

Test 2C: Analyse valve behaviour under two actuators failure

1. Set full flow
2. Generate a failure condition in two of the actuators
3. Impose 5 cycles of valve opening and closings, 2s open - 4s closed
4. Set turbine rotational speed to 2000 RPM

Measure current required per actuator	Open	Close	Actuator nr
actuator 1	[A] 2,0	[A] 1,6	2
actuator 2	[A] 1,9	[A] 1,7	4
actuator 3	[A] 1,9	[A] 1,7	
actuator 4	[A] 1,9	[A] 1,7	

Plot the input power received in the turbine vs. time (i.e. 2A)

Turn off the power electronics and check turbine runs down safely.

With full flow, check the rotor does not self-start under this condition.

OK / NOK
 OK / NOK

Test 2D: Analyse valve behaviour under three actuators failure

Not Possible to operate valve in these conditions.

Executed by IST Ana Casimiro Date: 11 / 5 / 2017
 Validated by Kymaner FOSSE JMANDETS Date: 11 / 5 / 2017
 Approved by Oceantec _____ Date: ____ / ____ / ____



Documento n.º/Document no.

OPE-100-PT-0008

Índice/Index

B

F/Sht

6

De/Of

8

Dry Lab Tests of PTO mechanical integrity + HSSV TOC

Test 2E: Analyse valve behaviour under air passage blockage

1. Blower and turbine are turned off
 2. Valve shutter is manually blocked with a wooden object preventing full closure
 3. Actuators signals should be recorded
 4. The contingency operation should be identified and tested - valve opens and closes several times
- Upon removal of the obstruction, valve resumes normal operation after resetting the system



OK / NOK

Test 2F: Cyclic loading/degradation

1. Set full flow on the blower
2. Set turbine rotational speed to 2000 RPM
3. Impose open and close operations cycles during 2h (T=1s)
4. Check system integrity and temperature of actuators

[°C]	40,2
[°C]	40,5
[°C]	39,8
[°C]	41,2

Measure maximum current required per actuator

- actuator 1
- actuator 2
- actuator 3
- actuator 4

[A]	2,1
[A]	2,2
[A]	2,6
[A]	2,6

Executed by IST Ana Gonçalves Date: 11 / 5 / 2017

Validated by Kymaner João Vaz Date: 11 / 5 / 2017

Approved by Oceantec _____ Date: ____ / ____ / ____



Documento n.º/Document no.

OPE-100-PT-0008

Índice/Index

F/Sht 7

B

De/Of 8